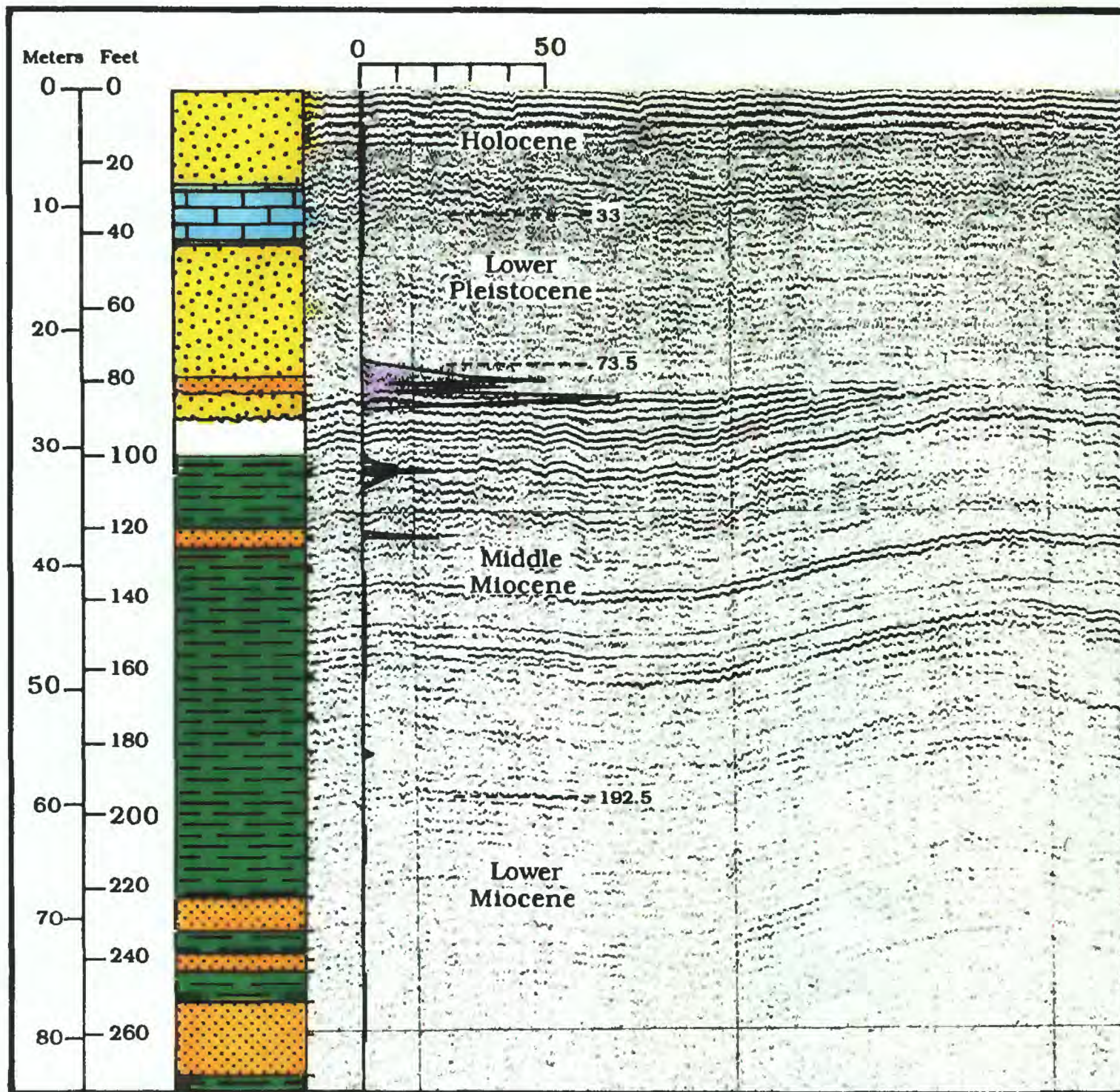


PHOSPHORITE POTENTIAL IN THE CONTINENTAL SHELF OFF GEORGIA: RESULTS OF THE TACTS CORE STUDIES

Open File Report 89-559



This report is preliminary and has not been reviewed for conformity with U.S. Geological Survey editorial standards and stratigraphic nomenclature.

Office of Energy and Marine Geology
Atlantic-Gulf Branch, Woods Hole, MA 02543



PHOSPHORITE POTENTIAL IN THE GEORGIA EEZ: PRELIMINARY RESULTS OF THE
TACTS CORE STUDIES

Edited by

F.T. Manheim

with contributions by

Paul F. Huddleston,	Georgia Geological Survey, Atlanta, Ga. 30334
Vernon J. Henry,	Georgia State University, Atlanta, Ga. 30334
Judith A. Commeau,	U.S. Geological Survey, Woods Hole, Mass. 02543
Jana L. Da Silva	U.S. Geological Survey, Woods Hole, Mass. 02543
Frank T. Manheim	U.S. Geological Survey, Woods Hole, Mass. 02543
Peter Popenoe	U.S. Geological Survey, Woods Hole, Mass. 02543
James R. Herring	U.S. Geological Survey, Denver, Co.

Table of Contents

	Page
I Introduction.....	1
II Location and core background data.....	4
by F.T. Manheim and J.R. Herring	
Table II-1. Locations and depths.....	6
Table II-2. Borehole designations.....	7
Table II-3. Sample register, Borehole A.....	8
Table II-4. Sample register, Borehole B.....	10
Table II-5. Sample register, Borehole C.....	12
Table II-6. Sample register, Borehole D.....	14
Table II-7. Sample register, Borehole E.....	16
Table II-8. Sample register, Borehole F.....	18
Table II-9. Sample register, Borehole G.....	20
Table II-10. Sample register, Borehole H.....	22
Table II-11. Total sample weights.....	24
Figure II-1. Location map.....	5
III Lithology of TACTS cores B, D, H, and AMCOR drillhole 6002 including optical estimates of phosphorite pellet concentrations.....	25
by F.T. Manheim, P.F. Huddlestun, and J.L. DaSilva	
Table III-1. Lithologic descriptions, Borehole B.....	34
Table III-2. Lithologic descriptions, Borehole D.....	38
Table III-3. Lithologic descriptions, Borehole H.....	41
Table III-4. Lithologic descriptions, AMCOR Hole 6002.....	45
Figure III-1. Core log, Borehole B.....	27
Figure III-2. Savannah Light Well.....	28
Figure III-3. Core log, Borehole D.....	29
Figure III-4. Core log, Borehole H.....	30
Figure III-5. Core log, AMCOR Hole 6002.....	31
Figure III-6. Stratigraphic profile of Savannah Light Well.....	32
Figure III-7. Microphotograph of phosphoritic sediment.....	33
IV Chemical analysis.....	50
By J.A. Commeau and F.T. Manheim	
Table IV-1. Chemical composition of sediment.....	52
Table IV-2. Comparison of chemical and volumetric analyses.....	53
V Regional summary of the geology of the miocene of Georgia and observations from the seismic data and TACTS cores.....	54
By P. Popenoe, P.F. Huddlestun and V.J. Henry	
Figure V-1. USGS tracklines and wells.....	55
Figure V-2. USGS and University of Georgia tracklines.....	56
Figure V-3. Cartoon depiction of early Miocene paleogeography.....	57
Figure V-4. Cartoon depiction of middle Miocene paleogeography.....	58
VI Summary and conclusions.....	62
VII References cited.....	63

Introduction

The Georgia shelf lies east of areas of phosphorite with near-commercial potential on the Georgia mainland and in the State territorial waters. It lies north and south of phosphatic Tertiary strata as indicated by shallow drill cores (Joint Oceanographic Institutions' Deep Earth Sampling Program - JOIDES) (Atlantic Margin Coring Project - AMCOR). However, except for the offshore Savannah Light boring and JOIDES hole 6002 (which has a relatively sparse sample coverage), little is known about sediments under the shelf.

The availability of new core data to about 100 m depth from eight sites on the middle Georgia shelf adds greatly to our knowledge of phosphorite distributions, general stratigraphy and ability to calibrate the existing offshore seismic network. These sites are the TACTS boreholes, drilled for the U.S. Navy by the McClelland Co. of Houston, Texas in 1984. The present report provides data on three coreholes. We offer detailed data of original samples and their available weights, locations, lithology and petrography, including volumetric estimates of phosphorite pellet content, chemical analyses, biostratigraphic age dating of the core holes, and a synthesis of regional geology of Georgia and its adjoining offshore area, including the paleogeography of the mid-Tertiary in the area. The remaining five coreholes are being processed at this writing. The work is a U.S. Geological Survey (USGS) contribution to the offshore Georgia Hard Minerals Task force and its attempt to evaluate the mineral potential in the EEZ area off Georgia.

Emergence of phosphorite potential off Georgia

The first evidence that phosphorite deposits off the Savannah, Georgia, might hold commercial potential and that these might be recovered competitive with existing land deposits in Florida and North Carolina were the Kerr-McGree lease requests to the State of Georgia and the Zellars-Williams economic analysis of 1979. The possible viability of offshore phosphorite recovery, which ran counter to widely held assumptions about offshore mining, was partly based on demographic changes and increased environmental/regulatory pressures and costs for onshore mineral recovery operations. A current economic evaluation (Zellars-Williams, 1988) offers an innovative technological scenario to permit offshore phosphorite mining by deep dredging (to as much as 50 m) coupled with an artificial-island preprocessing plant.

Significance of the North Carolina and Georgia offshore studies

Vibracore and seismic studies of S.R. Riggs and his coworkers off North Carolina drew attention to potential phosphorite deposits in the subsurface of Onslow Bay, North Carolina (Riggs, 1984; Marvasti and Riggs, 1987; Riggs and Manheim, 1988 and Riggs and others, 1985).

This development has importance for evaluation off Georgia Exclusive Economic Zone (EEZ) because the stratigraphic continuity of the North Carolina-Florida phosphatic middle Tertiary to and in the EEZ off Georgia has been suggested by various lines of evidences, including shallow seismic studies off Georgia by Kellam and Henry (1986) and Popenoe (1986); see also discussion in Ch. IV. However, interpretation of the seismic data has been handicapped by a lack of borehole information on paleontologic age, lithology, and phosphate distribution. Although the new Zellars-Williams report (1988) makes use of the USGS-seismic

reflection coverage of the area for compiling isopach maps of the Miocene and post-Miocene sediments (Popenoe and Spalding, 1988), no additional sediment verification beyond the earlier data from the Savannah Light well (Zellers-Williams, 1979) was utilized for maps that encompass the entire EEZ off Georgia. Only one other usable stratigraphic borehole, AMCOR 6002, was available until recently off the Georgia EEZ for ground verification purposes (Hathaway and others, 1979; Manheim and others, 1980, Poppe, 1981). Other borings didn't recover usable sediment samples.

Development of borehole mining systems applicable to deeper offshore phosphorite

An experimental borehole mining system initiated by the U.S. Bureau of mines and tested by AGRICO Co. (Scott, 1982; Savanick, 1985) demonstrated the technical feasibility of recovering deeper phosphorites to more than 100 m below sea floor where sufficient formation strength in upper layers permitted. This technique potentially opens up more than 10,000 km² of deeper strata to mineral recovery.

The possibility of control of turbidity by return of fines to the subsurface and minimal disturbance of the shelf surface is an additional, environmentally favorable attribute of the borehole mining technique, but its economic performance has not yet been tested.

The TACTS boreholes

In 1984, the U.S. Navy contracted for eight boreholes to be drilled for foundation evaluation purposes in the offshore Georgia area by the McClelland Co. of Houston, Texas. These Tactical Air Command Test Site (TACTS) borings were made available to the Branch of Atlantic Marine Geology of the U.S. Geological Survey and are stored at the Woods Hole Oceanographic Institution (WHOI) core and rock repository in Woods Hole, Mass.

Although the TACTS drill cores do not represent continuous coverage of penetrated strata (about 100 m), they are sited in key areas of the inner Georgia EEZ. After proposals and discussions in 1987, a cooperative study of the TACTS borings by the U.S. Geological Survey, Georgia Geological Survey, and Georgia State University was initiated in early 1988, sponsored by the U.S. Minerals Management Service, the U.S. Geological Survey, and the Bureau of Mines.

This report provides information on lithology, biostratigraphy, phosphate distribution and supporting chemical information on three Tacts boreholes, as well as interpretations of the regional geologic and resource significance of the new data. More extensive chemical and trace element information will be provided in a future report.

All of the paleontologic and stratigraphic subdivisions of the new core material are provided by Paul F. Huddlestun of the Georgia Geological Survey. The regional stratigraphic interpretation of these data is discussed cooperatively in Ch. IV.

Acknowledgements

We thank M. Cruickshank, formerly of USGS, Reston, Va., for assistance in acquiring the TACTS cores; Gary Skipp, USGS, Denver, for assistance in core sampling; P. Forrestel, D. Blackwood and D. Lubinski of the USGS, Woods Hole for help in preparing special illustrations; C.W. Poag of USGS, Woods Hole, for foraminiferal identifications; J. Broda and C.E. Franks of the Woods Hole Oceanographic Institution for assistance in accessing cores, and McClelland Co. of Houston, Texas, for background information and help regarding the TACTS cores. The financial support of the U.S. Minerals Management Service and Bureau of Mines is gratefully acknowledged.

II Location and core background data

By F. T. Manheim and J. R. Herring

The locations of most known drill cores in the EEZ section are depicted in Figure 1 and Table 1. However, only the TACTS, AMCOR, and (JOIDES) cores offer useful material for present purposes, since the other wells drilled through the key Neogene strata, recovering only cuttings that are not useful in evaluating economic potential. Geophysical logging generally encompassed only post-Neogene horizons.

The TACTS core materials exist in three forms: pint Mason jars of artificially consolidated materials left from physical properties tests such as triaxial compressive strength; intact core sections of a few inches to 1' in plastic tubes of 2.5" (6.5 cm) inner diameter; and bags of loose material, generally from near-surface sections. The cores are clearly the best preserved and best depth-defined. They have been used whenever a choice was available. They also experienced the least drying.

We created new designations for the TACTS boreholes to eliminate confusion between the Navy and McClelland numbering systems and to permit straightforward computer coding (Table 2). Tables 3-10 list the total available samples in the WHOI core repositories along with presampling weights. Of the eight boreholes, three, B, D and H (McClelland B-2, B-5 and B-7 respectively) were sampled in this study.

We can estimate roughly the proportion of the hole volume for which core was available by summing sample weights against the equivalent weight of total volume of the borehole core diameter (Table 11). The mean density of 6 samples used to estimate sediment density is 1.73. However, though they appeared fresh, the length and conditions of storage suggested that some evaporation has taken place. Therefore we computed a mean nonphosphatic bulk density of 1.667 from water content data in J-2 and J-1 (wells on the Florida shelf near the Georgia border). The formula used was:

$$D_{\text{sed}} = 1/[(1-W)G_{\text{sed}} + W]$$

where W is fractional water content (g/g) and G_{sed} is mineral grain density of nonphosphatic sediment, assumed to be 2.60 g/cm³. This value corresponds to a mean water content of 0.35 (35% wet weight) for the strata, which value was used later to convert between volume and weight units. Units are not salt-corrected.

Figure II-1. Location map for geological boreholes off Georgia and neighboring states. TACTS boreholes have single letter designations. For list of data on boreholes and cross-reference with earlier designations see Tables II-1 and II-2.

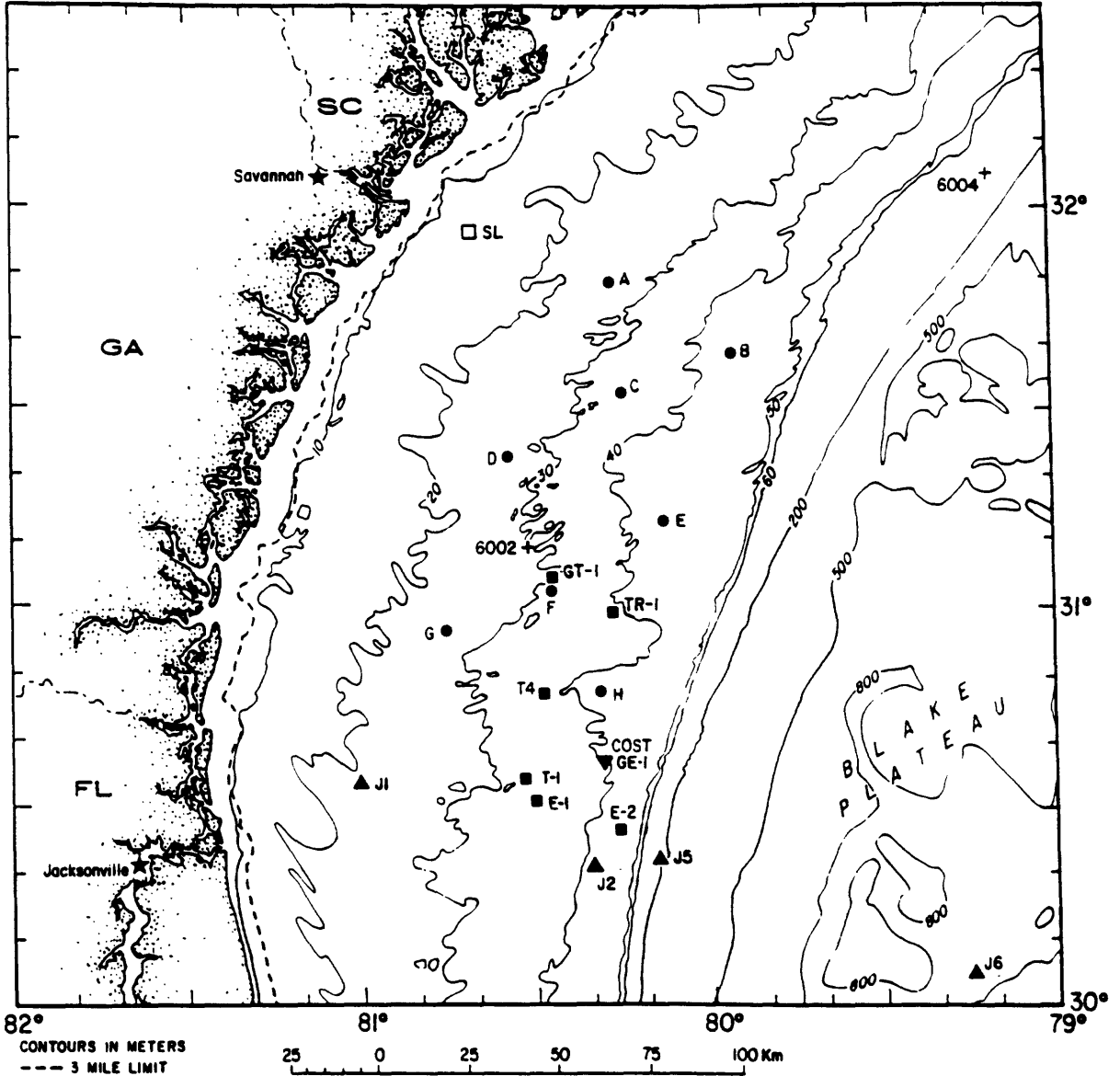


Table II-1. Location and other information for boreholes in Georgia and adjoining areas. Abbreviations are JOIDES: Joint Oceanographic Institutions Deep Earth Sampling Program (NSF); COST: Continental Offshore Stratigraphic Test (Scholle, 1979); AMCOR: Atlantic Continental Margin Coring Project 1976 (Hathaway and others, 1979); SL: Savannah Light boring, U.S. Coast Guard.

DATE	SITE NO.	LATITUDE	LONGITUDE	WATER DEPTH		PENETRATION DEPTH		ORIGINATOR
		(NORTH)	(WEST)	(M)	(FT)	(M)	(FT)	
1962-63	SL	31.948	80.666	16	52	47	154	U.S.C.G.
1965	J-1	30.550	81.000	25	82	277	910	JOIDES
1965	J-2	30.350	80.333	42	138	173	569	JOIDES
1965	J-5	30.383	80.133	190	623	245	804	JOIDES
1965	J-6	30.083	79.250	805	2,640	120	393	JOIDES
1976	6002	31.149	80.518	32	106	304	1,000	AMCOR
1976	6004	32.077	79.107	174	570	308	1,010	AMCOR
1979	T-1 +	30.790	80.473	35	115	2,292	7,518	TENNECO
1979	T-2 +	30.602	80.534	30	98	2,211	7,252	TENNECO
1979	GT-1+	31.080	80.442	35	115	2,070	6,790	GETTY
1979	TR-1+	30.999	80.251	40	131	3,475	11,398	TRANSCO
1979	E-1 +	30.577	80.509	32	105	2,249	7,377	EXXON
1979-80	E-2 +	30.444	80.260	139	455	3,850	12,628	EXXON
1979	GE-1	30.620	80.310	42	136	3,970	13,022	COST
1984	A	31.846	80.274	25	81†	98	321	U.S. NAVY*
1984	B	31.633	79.925	45	146†	91	300	U.S. NAVY*
1984	C	31.533	80.233	35	115†	102	336	U.S. NAVY*
1984	D	31.395	80.566	26	86†	98	323	U.S. NAVY*
1984	E	31.216	80.116	43	147†	92	302	U.S. NAVY*
1984	F	31.049	80.449	32	105†	100	329	U.S. NAVY*
1984	G	30.941	80.749	25	83†	97	319	U.S. NAVY*
1984	H	30.799	80.316	41	135†	97	319	U.S. NAVY*

† The depth of the TACTS core samples was given for mean low water, other the samples presumed mean sea level.

* By McClelland Company

+ No or marginal data known to be useful for phosphate evaluation at this time.

Table II-2. Cross reference, equivalents for TACTS core designations (see text).

USGS TACTS designation	McClelland TACTS designation	U.S. Navy TACTS designation
A	B-1	R-7
B	B-2	R-8
C	B-3	M2R6
D	B-5	R-2
E	B-4	R-3
F	B-6	M1R1
G	B-8	R-5
H	B-7	R-4

Table II-3. Total samples available in USGS core holdings for TACTS Borehole A cores prior to sampling. T refers to cores stored in tubes, B to bags all others jars.

USGS Sample ID (m)	Depth (ft)	McClelland Boring Design.	McClelland Sample Design.	Weight Sample (Kg)
A1.1	3.5	B1	S1	.10
A1.9	6.2	B1	S2	.00
A2.2	7.2	B1	S4	.00
A2.9	9.5	B1	S3	.15
A3.4	11.0	B1	S5	.36
A4.6	15.0	B1	S6	.22
A5.8	19.0	B1C	S1	3.20
A6.6	21.5	B1	S8	.15
A7.2	23.5	B1	S9	.18
A8.4	27.8	B1	S10	.00
A8.5	28.0	B1C	S2	3.49
A9.3	30.5	B1	S11	.16
A10.5	34.5	B1	S12	.20
A16.1	53.0	B1C	S3	2.78
A17.2	56.5	B1	S15	.15
A17.4	57.0	B1	S16	.16
A17.7	58.0	B1	S18	.10
A20.6	67.5	B1	S17	.22
A24.4	80.0	B1	S19	.25
A25.9	85.0	B1	S20	.16
A26.0	85.5	B1	S21	.10
A26.1	85.5	B1	S21	.46
A26.2	86.0	B1	S22	.30
A27.4	90.0	B1	S23	.64
A27.6	90.5	B1	S24	.45
A30.2	99.0	B1	S25	.32
A30.3	99.5	B1	S26	.20
A33.1	108.5	B1	S27	.45
A33.2	109.0	B1	S28	.30
A33.4	109.5	B1	S29	.46
A36.6	120.0	B1	S31	.71
A36.7	120.5	B1	S32	.22
A39.6	130.0	B1	S33	.15
A39.7	130.5	B1	S34	.10
A39.8	130.5	B1	S34	.48
A39.9	131.0	B1	S35	.41
A42.6	140.0	B1	S36	.45
A42.7	140.0	B1	S38	.25
A42.8	140.5	B1	S37	.90
A45.1	148.0	B1	S39	.10
A45.3	148.5	B1	S40	.15
A48.0	157.5	B1	S41	.23
A48.2	158.0	B1	S43	.23
A48.6	159.5	B1	S42	.71
A51.2	168.0	B1	S45	.08
A51.4	168.5	B1	S46	.35

A51.7	169.5	B1	S44	.87
A54.6	179.0	B1	S47	.30
A54.7	179.5	B1	S48	.47
A54.9	180.0	B1	S49	.25
A57.1	187.3	B1	S50	.00
A58.2	190.8	B1	S51	.35
A60.0	197.0	B1	S52	.10
A60.4	198.0	B1	S54	.22
A61.1	200.5	B1	S53	.96
A62.7	206.0	B1	S55	.70
A62.8	206.0	B1	S55	.15
A62.9	206.5	B1	S56	.23
A65.8	216.0	B1	S57	.43
A66.0	216.5	B1	S58	.30
A66.1	217.0	B1	S59	.20
A68.6	225.0	B1	S60	.44
A72.1	236.5	B1	S62	.98
A72.2	237.0	B1	S63	.42
A81.4	267.0	B1	S66	.97

Table II-4. Total samples available in USGS core holdings for TACTS Borehole B cores prior to sampling. T refers to cores (tubes); B to bags; all others, jars.

USGS Sample ID (m)	Depth (ft)	McClelland Boring Design.	McClelland Sample Design.	Weight Sample (Kg)
B0.2	0.5	B-2	S-1	.1
B1.4	4.5	B-2	S-2	.15
B2.4	7.8	B-2	S-3	.1
B2-9	10.0	B-2C	S-1B	.22
B3.0	10.0	B-2C	S-1B	.1
B3.1	10.5	B-2C	S-4	.65
B3.2	10.5	B2C	S-1B	.35
B3.3	10.5	B2	S-1C(a)	~0
B3.3	10.5	B2C	S-1C(b)	1.12
B4.1	13.5	B2	S-5	.1
B5.0	16.5	B2	S-6	.22
B5.4	18.0	B2C	S-2	1.36
B5.5	18.0	B2C	S-2	1.6
B5.9	19.5	B2	S-7	.1
B7.0	23.0	B2	S-8	.09
B7.9	26.0	B2	S-9	.22
B9.1	30.0	B2	S-10	.15
B10.0	33.0	B2	S-11	.65
B11.0	36.0	B2	S-12	.15
B12.2	40.0	B2	S-13	.5
B12.8	42.0	B2	S-14	.48
B14.8	48.5	B2	S-15	.2
B20.9	68.5	B2	S-17	.1
B24.1	79.0	B2	S-18	.46
B24.8	81.5	B2C	S-20	1.14
B30.6	100.5	B2	S-25	.3
B31.1	102.0	B2C	S-26	.38
B34.0	111.5	B2C	S-28	.88
B37.2	122.0	B2C	S-30	.68
B37.3	122.5	B2C	S-31	.05
B37.5	123.0	B2C	S-32	.3
B40.1	131.5	B2C	S-33	.31
B40.2	132.0	B2C	S-34	.9
B40.4	132.5	B2C	S-35	.3
B43.2	142.0	B2C	S-36	.2
B43.3	142.0	B2	S-37	.25
B43.6	143.0	B2C	S-38	.3
B46.2	151.5	B2	S-39	.25
B46.3	152.0	B2C	S-40	.3
B49.2	161.5	B2C	S-41	.2
B49.4	162.0	B2C	S-42	.68
B49.5	162.5	B2C	S-43	.25
B49.6	162.5	B2C	S-43	.1
B52.4	172.0	B2C	S-44	.22
B52.6	172.5	B2C	S-45	.15
B52.7	172.8	B-2C	S-45	.1

B52.8	173.0	B-2C	S-46	.35
B55.6	182.5	B-2C	S-47	.88
B55.8	183.0	B-2C	S-48	.17
B58.5	192.0	B-2C	S-49	.92
B58.7	192.5	B-2	S-50	.25
B58.8	193.0	B-2C	S-51	.46
B61.6	202.0	B-2C	S-52	1.1
B61.8	202.5	B-2C	S-53	.14
B64.6	212.0	B-2C	S-54	.23
B64.8	212.5	B-2C	S-55	1.0
B64.9	213.0	B-2C	S-56	.43
B67.7	222.0	B-2C	S-57	.79
B67.8	222.5	B-2	S-58	.22
B68.0	223.0	B-2C	S-58	.44
B70.4	231.0	B-2C	S-60	.75
B70.6	231.5	B-2	S-61	.43
B70.7	232.0	B-2C	S-62	.3
B73.2	240.0	B-2C	S-63	.21
B73.6	241.5	B-2C	S-64	.89
B73.8	242.0	B-2C	S-65	.43
B76.2	250.0	B-2C	S-66	.7
B76.4	250.5	B-2C	S-67	.98
B76.5	251.0	B-2C	S-68	.3
B79.2	260.0	B-2C	S-66	.16
B79.4	260.5	B-2	S-70	.38
B79.6	261.0	B-2C	S-71	.47
B82.3	270.0	B-2C	S-72	.69
B82.4	270.5	B-2	S-73	.19
B82.6	271.0	B-2C	S-74	.35
B85.0	279.0	B-2C	S-75	.23
B85.2	279.5	B-2C	S-76	.9
B85.6	281.0	B-2C	S-77	.3
B88.1	289.0	B-2C	S-78	.82
B88.2	289.5	B-2	S-79	.38
B88.4	290.0	B-2C	S-80	.23
B91.1	299.0	B-2C	S-81	.2
B91.3	299.5	B-2C	S-82	.97
B91.4	300.0	B-2C	S-83	.46

Table II-5. Total samples available in USGS core holdings for TACTS Borehole C cores prior to sampling. T refers to cores (tubes), B to bags, all others, jars.

USGS Sample ID (m)	Depth (ft)	McClelland Boring Design.	McClelland Sample Design.	Weight Sample (Kg)
C0.2	0.5	B-3	S-1	.15
C1.5	1.5-2.1	B-3	P-1,B	.15
C3.2	10.5	B-3	S-3	.1
C4.1	13.5	B-3	S-4	.16
C5.0	16.5	B-3	S-5	.07
C5.3	17.5	B-3	S-8A	.68
C5.6	18.5	B-3	S-6	.3
C6.6	21.5	B-3	S-7	.2
C7.8	25.5	B-3	S-9	.1
C8.7	28.5	B-3	S-10	.1
C9.3	30.5	B-3	S-11	.4
C10.4	34.0	B-3	S-12	.16
C11.0	36.0	B-3	---,B	1.45
C11.3	37.0	B-3	S-13	.16
C12.2	40.0	B-3	S-14	.22
C14.0	46.0	B-3	S-15	.24
C14.8	48.5	B-3	S-15	.20
C17.7	58.0	B-3C	S-17	.87
C17.8	58.5	B-3	S-18	.46
C18.0	59.0	B-3C	S-19	.30
C20.7	68.0	B-3C	S-20	.90
C20.9	68.5	B-3	S-21	.25
C21.0	69.0	B-3C	S-22	.48
C23.8	78.0	B-3C	S-23	.70
C23.9	78.5	B-3	S-24	.36
C24.1	79.0	B-3C	S-25	.38
C26.4	86.5	B-3C	S-26	.94
C26.7	87.5	B-3	S-27	.26
C26.8	88.0	B-3C	S-28	.47
C29.1	95.5	B-3C	S-29	.46
C29.3	96.0	B-3C	S-30	.40
C32.3	106.0	B-3C	S-31	.68
C32.5	106.5	B-3	S-32	.35
C32.6	107.0	B-3C	S-33	.27
C35.1	115.0	B-3C	S-34	.68
C35.2	115.5	B-3C	S-35	.38
C35.4	116.0	B-3C	S-36	.40
C37.2	122.0	B-3C	S-37	.70
C37.3	122.5	B-3	S-38	.30
C37.5	123.0	B-3C	S-39	.44
C40.5	133.0	B-3C	S-40	1.0
C40.7	133.5	B-3C	S-41	.30
C40.8	134.0	B-3C	S-42	.47
C43.9	144.0	B-3	S-43	.40
C44.0	144.5	B-3	S-44	.25

C46.6	153.0	B-3C	S-45	.05
C50.1	164.5	B-3C	S-46	.45
C50.3	165.0	B-3C	S-47	.42
C53.3	175.0	B-3C	S-48	.89
C53.5	175.5	B-3C	S-49	.41
C53.6	176.0	B-3C	S-50	.45
C56.4	185.0	B-3C	S-51	.90
C56.5	185.5	B-3C	S-52	.50
C56.7	186.0	B-3B	S-53	.47
C59.4	195.0	B-3C	S-54	1.0
C59.6	195.5	B-3	S-55	.43
C59.7	196.0	B-3C	S-56	.38
C62.2	204.0	B-3C	S-57	1.0
C62.3	204.5	B-3C	S-58	.50
C65.5	205.0	B-3C	S-59	.44
C65.3	214.0	B-3	S-60	.99
C65.4	214.5	B-3	S-61	.45
C65.5	215.0	B-3C	S-62	.45
C68.0	223.0	B-3C	S-63	1.0
C68.1	223.5	B-3C	S-64	.44
C68.3	224.0	B-3C	S-65	.48
C71.6	235.0	B-3C	S-66	1.09
C71.8	235.5	B-3C	S-67	.63
C71.9	236.0	B-3C	S-68	.40
C73.8	242.0	B-3C	S-69	1.0
C73.9	242.5	B-3	S-70	.45
C74.1	243.0	B-3C	S-71	.46
C76.8	252.0	B-3C	S-72	.99
C77.0	252.5	B-3C	S-73	.45
C77.1	253.0	B-3C	S-74	.50
C78.0	262.0	B-3C	S-75	.90
C80.0	262.5	B-3C	S-76	1.10
C80.2	263.0	B-3	S-77	.10
C82.9	272.0	B-3C	S-78	.98
C83.1	272.5	B-3C	S-79	1.0
C83.2	273.0	B-3C	S-80	.16
C86.9	285.0	B-3C	S-84	.39
C87.0	285.5	B-3	S-81	.21
C87.2	286.0	B-3C	S-82	.40
C89.8	294.5	B-3C	S-83	.46
C96.0	315.0	B-3C	S-85	1.0
C96.2	315.5	B-3	S-86	.41
C96.3	316.0	B-3C	S-87	.44
C102.1	335.0	B-3C	S-88	1.10
C102.3	335.5	B-3	S-89	.43
C102.4	102.4	B-3C	S-90	.48

Table II-6. Total samples available in USGS core holdings for TACTS Borehole D cores prior to sampling. T refers to cores (tubes); B to bags; all others, jars.

USGS Sample ID (m)	Depth (ft)	McClelland Boring Design.	McClelland Sample Design.	Weight Sample (Kg)
D0.3	1.0	B-5	S-6	.16
D0.7	2.4	B-5	S-7	.14
D1.5	5.0	B-5	S-8	.45
D2.7	9.0	B-5	S-11	.43
D4.3	14.0	B-5	S-13	.15
D5.2	17.0	B-5	S-14	.26
D6.9	22.5	B-5	S-16	.20
D8.8	29.0	B-5	S-18	.38
D9.4	31.0	B-5	S-17	3.40
D10.7	35.0	B-5	S-20	.45
D10.8	35.5	B-5	S-21	.1
D10.8	35.5	B-5	S-21	.9
D11.6	38.0	B-5	S-22	1.1
D11.7	38.5	B-5	S-23	.2
D14.2	46.5	B-5	S-1	.66
D14.3	47.0	B-5	S-2	.4
D17.8	58.5	B-5	S-3	.35
D18.0	59.0	B-5	S-4	.5
D18.1	59.5	B-5	S-5	.24
D18.4	60.5	B-5	S-24	.2
D21.3	70.0	B-5	S-25	.1
D21.5	70.5	B-5	S-26	1.0
D21.6	71.0	B-5	S-27	.3
D24.4	80.0	B-5	S-28	.23
D24.5	80.5	B-5	S-29	.45
D24.7	81.0	B-5	S-30	.26
D27.4	90.0	B-5	S-31	.7
D27.6	90.5	B-5	S-32	.25
D27.7	91.0	B-5	S-33	.3
D30.5	100.0	B-5	S-34	.14
D33.5	110.0	B-5	S-35	.32
D33.7	110.5	B-5	S-36	.89
D33.8	111.0	B-5	S-37	.23
D36.9	121.0	B-5	S-38	.12
D37.0	121.5	B-5	S-39	.45
D37.1	121.5	B-5	S-39	.07
D37.5	123.0	B-5	S-40	.21
D39.8	130.5	B-5	S-41	.25
D39.9	131.0	B-5	S-42	.16
D43.9	144.0	B-5	S-43	.16
D44.0	144.5	B-5	S-44	1.0
D44.2	145.0	B-5	S-45	.3
D46.9	154.0	B-5	S-46	1.1
D47.1	154.5	B-5	S-47	.44
D48.9	160.5	B-5	S-48A	.5
D49.1	161.0	B-5	S-49	.15

D52.7	173.0	B-5	S-50	.15
D52.9	173.5	B-5	S-51A	.2
D52.9	173.5	B-5	S-51B	.11
D53.0	174.0	B-5	S-52	.23
D55.6	182.5	B-5	S-53	.7
D55.8	183.0	B-5	S-54	.42
D55.9	183.5	B-5	S-55	.25
D58.8	193.0	B-5	S-56	1.0
D59.0	193.5	B-5	S-57	.45
D61.6	202.0	B-5	S-73	.21
D61.7	202.5	B-5	S-59	.14
D63.9	209.5	B-5	S-60	.45
D64.3	211.0	B-5	S-61	.21
D66.6	218.5	B-5	S-62	.68
D70.0	229.5	B-5	S-63	.38
D70.3	230.5	B-5	S-64	.1
D73.3	240.5	B-5	S-65	.05
D76.4	250.5	B-5	S-66	.25
D79.4	260.5	B-5	S-68	.41
D79.6	261.0	B-5	S-69	.2
D82.8	271.5	B-5	S-70	.2
D82.9	272.0	B-5	S-71	.21
D85.8	281.5	B-5	S-72	.22
D91.0	298.5	B-5	S-74	.18
D91.1	299.0	B-5	S-75	.3
D98.3	322.5	B-5	S-76	.2
D98.5	323.0	B-5	S-77	.22

Table II-7. Total samples available in USGS core holdings for TACTS Borehole E cores prior to sampling. T refers to cores (tubes); B to bags; all others, jars.

USGS Sample ID (m)	Depth (ft)	McClelland Boring Design.	McClelland Sample Design.	Weight Sample (Kg)
E4.6	15.0	B-4C	S-1	1.6
E5.5	18.0	B-4	S-7	.45
E10.7	35.0	B-4	S-14	.46
E11.6	38.0	B-4	S-15	.36
E12.5	41.0	B-4	S-16	.21
E14.6	48.0	B-4	S-17	.18
E17.7	58.0	B-4	S-18	.5
E23.5	77.0	B-4	S-20	.39
E26.5	87.0	B-4	S-21	.40
E29.4	96.5	B-4	S-22	.30
E29.6	97.0	B-4	S-23	.5
E32.6	107.0	B-4	S-24	.45
E35.7	117.0	B-4	S-25	.44
E35.8	117.5	B-4	S-26	.23
E36.0	118.0	B-4	S-27	.22
E38.7	127.0	B-4	S-28	.24
E41.8	137.0	B-4	S-29	.42
E44.8	147.0	B-4	S-30	.40
E48.0	157.5	B-4	S-31	.28
E48.2	158.0	B-4	S-32	.44
E51.1	167.5	B-4	S-33	.16
E54.4	178.5	B-4	S-34	.40
E54.6	179.0	B-4	S-35	.28
E57.8	189.5	B-4	S-36	.85
E57.9	190.0	B-4	S-37	.1
E60.7	199.0	B-4	S-38	.23
E60.8	199.5	B-4	S-39	1.0
E61.0	200.0	B-4	S-40	.30
E64.5	211.5	B-4	S-41	.60
E64.6	212.0	B-4	S-42	.15
E67.1	220.0	B-4	S-43	.90
E67.2	220.0	B-4	S-44	.23
E67.4	221.0	B-4	S-45	.22
E70.0	229.5	B-4	S-46	.43
E70.1	230.0	B-4	S-47	.15
E73.0	239.5	B-4	S-48	.25
E73.3	240.5	B-4	S-50	.22
E76.0	249.5	B-4	S-51	.45
E76.2	250.0	B-4	S-52	.23
E76.3	250.3	B-4	S-53	.28
E79.1	259.5	B-4	S-54	.40
E79.2	260.0	B-4	S-55	.39
E82.1	269.5	B-4	S-56	.25
E82.4	270.5	B-4	S-57	.35
E82.6	271.0	B-4	S-58	.35
E85.6	281.0	B-4	S-59	.28

E88.5	290.5	B-4	S-60	.46
E88.7	291.0	B-4	S-61	.20
E91.4	300.0	B-4	S-62	.30
E91.6	300.5	B-4	S-63	.85
E91.8	301.3	B-4	S-64	.22

Table II-8. Total samples available in USGS core holdings for TACTS Borehole F cores prior to sampling. T refers to cores (tubes); B to bags; all others, jars.

USGS Sample ID (m)	Depth (ft)	McClelland Boring Design.	McClelland Sample Design.	Weight Sample (Kg)
F0.1	0.3	B-6	S-13A,B	.22
F0.2	0.5	B-6	S-1	.22
F2.9	9.5	B-6	S-3	.11
F3.4	11.0	B-6	S-4	.65
F5.8	19.0	B-6	S-6	1.45
F5.9	19.0	B-6	S-7	.43
F6.7	22.0	B-6	S-8	.31
F7.0	23.0	B-6	S-9	.43
F8.0	26.1	B-6	S-10	~0
F10.1	33.0	B-6	S-12	.43
F12.0	39.5	B-6	S-13B	.39
F12.2	40.0	B-6	S-13C	.15
F18.9	62.0	B-6	S-16(a)	1.0
F18.9	62.0	B-6	S-16(b)	.7
F19.0	62.0	B-6	S-16	1.16
F20.6	67.5	B-6	S-18	1.1
F23.8	78.0	B-6	S-20	.98
F23.9	78.5	B-6	S-21	1.2
F27.0	88.5	B-6	S-24	.5
F30.2	99.0	B-6	S-26	.69
F30.3	99.5	B-6	S-27	.41
F33.4	109.5	B-6	S-30	.35
F36.3	119.0	B-6	S-32	.68
F36.4	119.5	B-6	S-33	.3
F39.3	129.0	B-6	S-35	.68
F39.5	129.5	B-6	S-36	.35
F42.7	140.0	B-6	S-38	.18
F42.8	140.5	B-6	S-39	1.0
F43.0	141.0	B-6	S-40	.39
F45.7	150.0	B-6	S-41	.7
F45.9	150.5	B-6	S-42	.45
F46.0	151.0	B-6	S-43	.35
F48.8	160.0	B-6	S-44	.34
F48.9	160.5	B-6	S-45	1.1
F49.1	161.0	B-6	S-46	.28
F52.0	170.5	B-6	S-48	1.09
F52.1	171.0	B-6	S-49	.29
F55.0	180.5	B-6	S-50	.51
F55.2	181.0	B-6	S-51	.5
F58.1	190.5	B-6	S-52	.49
F58.2	191.0	B-6	S-53	.3
F61.4	201.5	B-6	S-54	.22
F61.6	202.0	B-6	S-55	.7
F61.7	202.5	B-6	S-56	.27

F64.0	210.1	B-6	S-57	.15
F67.1	220.0	B-6	S-58	.13
F67.2	220.5	B-6	S-59	.44
F67.4	221.0	B-6	S-60	.17
F70.1	230.0	B-6	S-61	.22
F70.3	230.5	B-6	S-62	.9
F70.4	231.0	B-6	S-63	.19
F72.8	239.0	B-6	S-64	.9
F73.0	239.5	B-6	S-65	.42
F73.1	240.0	B-6	S-66	.24
F75.9	249.0	B-6	S-67	1.09
F76.0	249.5	B-6	S-68	.23
F76.2	250.0	B-6	S-69	.22
F78.9	259.0	B-6	S-71	.44
F79.1	259.5	B-6	S-70	.90
F79.2	259.5	B-6	S-72	.25
F81.7	268.0	B-6	S-73	.95
F81.8	268.5	B-6	S-74	.46
F82.0	269.0	B-6	S-75	.45
F84.7	278.0	B-6	S-76	1.1
F84.9	278.5	B-6	S-77	.46
F85.0	279.0	B-6	S-78	.44
F87.5	287.0	B-6	S-79	.24
F87.6	287.5	B-6	S-80	.22
F87.8	288.0	B-6	S-81	.29
F93.6	307.0	B-6	S-82	.42
F93.7	307.5	B-6	S-83	.16
F99.8	327.5	B-6	S-84	1.18
F110.0	328.0	B-6	S-85	.46
F100.1	328.5	B-6	S-86	.9
F100.3	329.0	B-6	S-87	.2

Table II-9. Total samples available in USGS core holdings for TACTS Borehole G cores prior to sampling. T refers to cores (tubes); B to bags; all others, jars.

USGS Sample ID (m)	Depth (ft)	McClelland Boring Design.	McClelland Sample Design.	Weight Sample (Kg)
G0.3	1.0	B-8	S-1	.21
G0.9	3.0	B-8	S-4	.45
G1.8	6.0	B-8	S-5	.23
G2.7	9.0	B-8	S-6	.45
G4.3	14.0	B-8	S-7	.5
G4.9	16.0	B-8	S-8	.05
G5.0	16.3	B-8	S-9(a)	.9
G5.0	16.3	B-8	S-9(b)	1.1
G5.0	16.3	B-8	S-9(c)	.45
G5.2	17.0	B-8	S-10	.21
G5.6	18.5	B-8	S-11	.15
G5.8	19.0	B-8	S-12	.47
G6.4	21.0	B-8	S-13	.07
G7.6	25.0	B-8	S-14	.65
G8.5	28.0	B-8	S-15	.3
G9.3	30.5	B-8	S-16	.23
G10.7	35.0	B-8	S-18	.14
G11.3	37.0	B-8	S-19	.4
G14.0	46.0	B-8	S-20	.25
G17.1	56.0	B-8	S-21	.48
G19.8	65.0	B-8	S-22	.48
G22.9	75.0	B-8	S-23	.42
G25.9	85.0	B-8	S-24	.22
G29.0	95.0	B-8	S-25	.21
G32.0	105.0	B-8	S-26	.21
G35.1	115.0	B-8	S-27	.1
G35.2	115.0	B-8	S-27	.25
G38.1	125.0	B-8	S-28	.24
G41.0	134.5	B-8	S-29	.45
G41.1	135.0	B-8	S-30	.1
G44.2	145.0	B-8	S-31	.45
G47.5	156.0	B-8	S-32	.39
G50.6	166.0	B-8	S-33	.42
G53.6	176.0	B-8	S-34	.19
G56.7	186.0	B-8	S-35	.2
G60.0	197.0	B-8	S-36	.15
G63.4	208.0	B-8	S-37	.25
G63.6	208.5	B-8	S-38	.5
G63.7	209.0	B-8	S-39	.47
G66.0	216.5	B-8	S-1	.5
G66.1	217.0	B-8	S-2	.21
G66.4	218.0	B-8	S-40	.3
G66.8	219.0	B-8	S-42	.49
G66.9	219.5	B-8	S-41	.43
G67.1	220.0	B-8	S-P1	1.95
G69.5	228.0	B-8	S-43	.98

G69.6	228.5	B-8	S-44	.99
G69.8	229.0	B-8	S-45	.22
G72.7	238.5	B-8	S-46	.1
G72.8	239.0	B-8	S-47	.9
G73.0	239.5	B-8	S-48	.23
G75.9	249.0	B-8	S-49	.8
G76.0	249.5	B-8	S-50	.4
G76.2	250.0	B-8	S-51	.29
G78.8	258.5	B-8	S-52	.14
G78.9	259.0	B-8	S-53	1.07
G79.2	260.0	B-8	S-54	.17
G82.0	269.0	B-8	S-55	.9
G82.1	269.0	B-8	S-55	.15
G82.3	270.0	B-8	S-57	.39
G84.9	278.5	B-8	S-58	1.0
G85.0	279.0	B-8	S-59	.37
G85.1	279.3	B-8	S-60	.44
G87.9	288.5	B-8	S-61	.7
G88.1	289.0	B-8	S-62	.22
G88.2	289.3	B-8	S-63	.23
G91.0	298.5	B-8	S-64	1.0
G91.2	299.3	B-8	S-66	.3
G93.6	307.0	B-8	S-68	.23
G93.7	307.5	B-8	S-67	.47
G94.0	308.5	B-8	S-69	.21
G96.8	317.5	B-8	S-70	.9
G96.9	318.0	B-8	S-71	.38
G97.1	318.5	B-8	S-72	.17

Table II-10. Total samples available in USGS core holdings for TACTS Borehole H cores prior to sampling. T refers to cores (tubes); B to bags; all others, jars.

USGS Sample ID (m)	Depth (ft)	McClelland Boring Design.	McClelland Sample Design.	Weight Sample (Kg)
H1.2	4.0	B-7	S-1	2.5
H1.7	5.5	B-7	S-3	.19
H4.7	15.5	B-7	S-6	.05
H7.5	24.5	B-7	S-9	.45
H11.1	36.5	B-7	S-13	.1
H12.2	40.1	B-7	S-14	~0
H13.6	44.5	B-7	S-15	~0
H14.6	48.0	B-7C	S-2	1.0
H15.8	52.0	B-7	S-16	.52
H18.9	62.0	B-7	S-17	.33
H21.9	72.0	B-7	S-18	.28
H25.6	84.0	B-7	S-19	.36
H28.7	94.0	B-7	S-20	.28
H31.9	104.5	B-7	S-21	.37
H34.4	113.0	B-7	S-22	.11
H37.6	123.5	B-7	S-24	1.1
H37.8	124.0	B-7	S-25	.22
H40.5	133.0	B-7	S-26	.9
H40.7	133.5	B-7	S-27	1.06
H40.8	134.0	B-7	S-28	.42
H43.3	142.0	B-7	S-29	.85
H43.4	142.5	B-7	S-30	.85
H43.6	143.0	B-7	S-31	.22
H46.3	152.0	B-7	S-32	.98
H46.5	152.5	B-7	S-33	.44
H46.6	153.0	B-7	S-34	.4
H49.4	162.0	B-7	S-35	.93
H49.5	162.5	B-7	S-36	1.0
H49.7	163.0	B-7	S-37	.15
H52.1	171.0	B-7	S-38	.5
H52.4	172.0	B-7	S-39	.27
H55.2	181.0	B-7	S-40	.65
H55.4	182.0	B-7	S-41	.5
H58.2	191.0	B-7	S-42	.38
H58.4	191.5	B-7	S-43	.98
H58.5	192.0	B-7	S-44	.47
H58.7	192.5	B-7	S-45	.43
H59.0	193.5	B-7	S-46	.24
H61.0	200.0	B-7	S-47	1.0
H61.1	200.5	B-7	S-48	1.1
H61.3	201.0	B-7	S-49	.45
H66.6	218.5	B-7	S-83?	.3
H66.8	219.0	B-7	S-54	.1
H69.8	229.0	B-7	S-57	.45
H70.0	229.5	B-7	S-58	.23
H70.4	231.0	B-7	S-59	.9

H70.6	231.5	B-7	S-60	.9
H70.7	232.0	B-7	S-61	.24
H72.8	239.0	B-7	S-62	.9
H73.0	239.5	B-7	S-63	.9
H75.9	249.0	B-7	S-65	.23
H78.9	259.0	B-7	S-68	.9
H82.0	269.0	B-7	S-70	.9
H82.1	269.5	B-7	S-71	.23
H85.0	279.0	B-7	S-73	.9
H85.2	279.5	B-7	S-74	1.0
H85.3	280.0	B-7	S-75	.21
H88.1	289.0	B-7	S-76	.9
H88.2	289.5	B-7	S-77	.3
H91.1	299.0	B-7	S-79	.47
H94.2	309.0	B-7	S-81	.9
H94.3	309.5	B-7	S-82	.32
H97.2	319.0	B-7	S-84	.18

Table II-11. Proportion of boreholes sampled. Nominal weight (kg) = $D\pi r^2 L/1000$ where D = mean density (1.73), r = 3.175 cm, and L = length in cm.

Borehole	Total Sample Weight (Kg)	Length (Ft)	Length (Cm)	Nominal Weight (Kg)	Total Sample Wt./ Nominal Weight = %
A	29.16	236.5	8034	432.5	6.7
B	36.46	299.5	9131	491.6	7.4
C	50.82	355.5	10228	550.7	9.2
D	28.82	322.0	9817	528.5	5.5
E	18.71	386.3	8728	469.9	3.9
F	38.82	328.8	10022	539.6	7.2
G	22.61	317.5	9679	521.1	4.3
H	34.49	315.0	9603	517.0	6.7

III Lithology and phosphorite pellet concentration of TACTS cores B, D, H, and AMCOR drillhole 6002

By F. T. Manheim, P. F. Huddlestun, and J. L. Da Silva

Tables III-1-5 provide the lithologic descriptions for the Savannah Offshore drillhole, Tacts boreholes B, D, H, and AMCOR Hole 6002. The information given is based on visual descriptions using a binocular microscope, along with supplementary use of acid and the molybdate qualitative phosphate test. The information on AMCOR Hole 6002 was taken from previous data of the Atlantic Margin Coring Project (AMCOR) of the U.S. Geological Survey (Hathaway and others 1976, and unpublished data on file at the USGS offices in Woods Hole, Mass.). Figures III-1-6 display the lithology, the pellet concentrations, and the stratigraphy of the boreholes mentioned above. All stratigraphic units for the TACTS cores were determined by P. Huddlestun on the basis of foraminiferal zones.

The phosphorite pellet concentrations of TACTS Boreholes B, D, and H were visually estimated by counting pellets within a 100-cell grid area. Comparison with chemical data is facilitated by volumetric to weight/weight unit conversion factors provided in Chapter IV. We used composite analyses of pure carbonate fluorapatite apatite from marine phosphorites in the North Carolina area as a standard reference material (Van Kauwenbergh and McClellan, 1985). Color was judged by eye and grain-size estimates were made wet under the microscope. Sizes are referred to the standard Wentworth size ranges. Clay denotes unconsolidated material, whereas shale indicates partial consolidation and incipient fissility.

Phosphorite pellets were found in matrices of all types: sand, silt, shale and clay, and carbonate. However, the highest concentrations were observed at unconformities where interfaces of several lithologies are found. Lowest concentrations were observed in sediments that had high concentrations of calcium carbonate. The pellets in pre-Pliocene strata were generally brown-black, vitreous ovoids, often having consistent grain diameters in the range of 0.1 to 0.3 mm. Larger grain aggregates, often with gray-black color, were mainly found in post-middle Miocene sediments and may be attributed to recementation and reworking.

The phosphatic nature of the pellets was verified by qualitative chemical tests whenever there was uncertainty during visual analysis. However, they may contain extraneous material, i.e., may not be 100 percent carbonate fluorapatite (CFA), as assumed in the conversion formulae. The water content of the pellets was also assumed to be 0 without verification, although pellets had a nonporous, vitreous appearance, suggesting low water content.

The silts and clays of the main Middle to Lower Miocene formations were characterized by olive-green silts and clays having significant foraminiferal content, both benthic and pelagic. Glauconite was relatively rare. Dolomite was frequently present but has not been systematically reported here.

The phosphate peaks on the well logs were drawn to a baseline represented by the midpoint to the next data points. This tends to reduce exaggeration of peak importance (width) where samples are sparse, but exaggeration may remain in many cases. In other cases, however, unrecorded peaks may exist where we had no sample coverage. The lithologic symbol pattern has been chosen on a "best estimate" basis for the most part, but in some areas, white space denotes uncertain lithology.

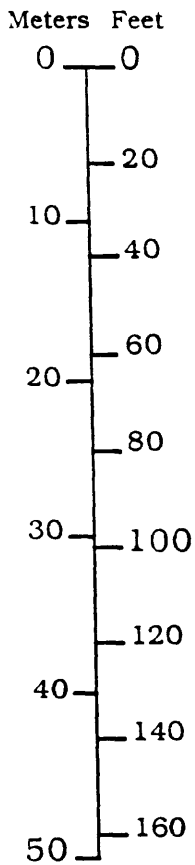
Highly phosphatic sediments below the middle Miocene unconformity were often dark and organic-appearing, whether they were in clays, silts, or sands. Further, many emitted a petroleum-like smell upon acid addition. This corresponds to a finding of tarry substance in correlative strata from the J-2 well (Charm and others, 1969; see also further comments in Ch. IV). Gypsum in the form of shining crystals was frequently found in the samples, especially those that were dried out. This finding cannot be due to evaporation of pore water because gypsum far exceeds in bulk the sulfate ($<0.27\% \text{SO}_4$ in seawater) that could be supplied in original porosity. The fact that the presence of gypsum is well correlated to drying of samples, microrupturing of sediment structure by small crystal balls after the core was recovered, and the brilliant, unleached quality of crystallites all point to its main origin as an artifact. Thus, we presume that most gypsum would be due to postsampling decomposition of iron sulfide (pyrite), its oxidation and subsequent reaction of the sulfuric acid formed from sulfide with local carbonate. The corrosion of carbonates in some of the high-gypsum samples supports this conclusion. However, bearing in mind the subaerial exposure of the upper strata during Pleistocene emergence, formation of localized evaporitic ponds in Pleistocene time cannot be excluded.

Finally, some comment on the origin of the phosphorite is appropriate. The pelletal phosphorite is clearly associated with Miocene formations and, through its uniform dark color and size within a given depth sequence, appears to be a primary deposit. Some foraminifera contained internal micropellets, suggesting that at least some pellets were formed as molds inside the carbonate organisms. In contrast, phosphorites occurring above the Miocene boundary were dominated by irregular forms that were often larger than .3 mm and frequently variable in degree of phosphatization.

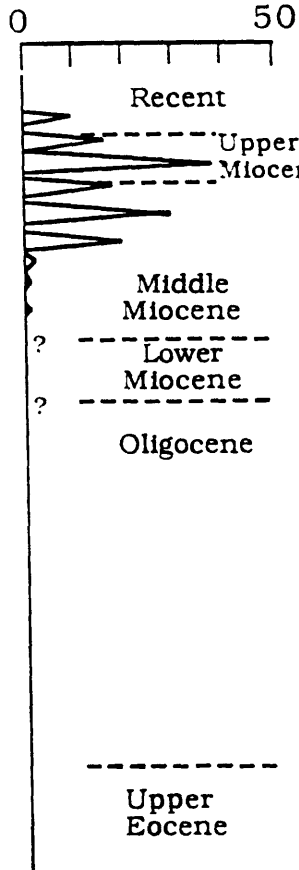
Figure III-1. Lithologic log for Savannah Offshore Light well, redrawn from data of McCollum and Herrick, 1967, and Zellars-Williams, 1979. Phosphorite pellet equivalents computed from BPL data (see text and Chapter V, this report); other data, as in text to Fig. III-2.

Savannah Light Tower

Depth



Phosphate (% pellets)



Lithology

Recent
Quartz sand and silt, fossiliferous

Upper Miocene
Fine sand and silty clay, olive-green, containing varying amounts of medium to fine-grained phosphorite pellets

Middle Miocene
Silty clay, greenish-gray, sparsely phosphatic
Sandy limestone, sparsely phosphatic

Lower Miocene
Sandy limestone, phosphatic, shelly

Oligocene
Limestone, white to cream, sandy in part, fossiliferous

Upper Eocene
Limestone, gray to buff, highly fossiliferous

Figure III-2. Lithologic log for Tacts Borehole B. Ticks and bars along the right side of the lithology column refer to location and extent of samples. Dots - sand; fine dots = silt; short dashed line = silty-clay; lines = clay or shale; brick pattern - carbonate. In stratigraphic column letters refer to standard paleontologic time zones. Phosphate concentrations are estimated volumetrically by methods described in text. Source data under "Lithology" given in core description, Table 1.

BOREHOLE B

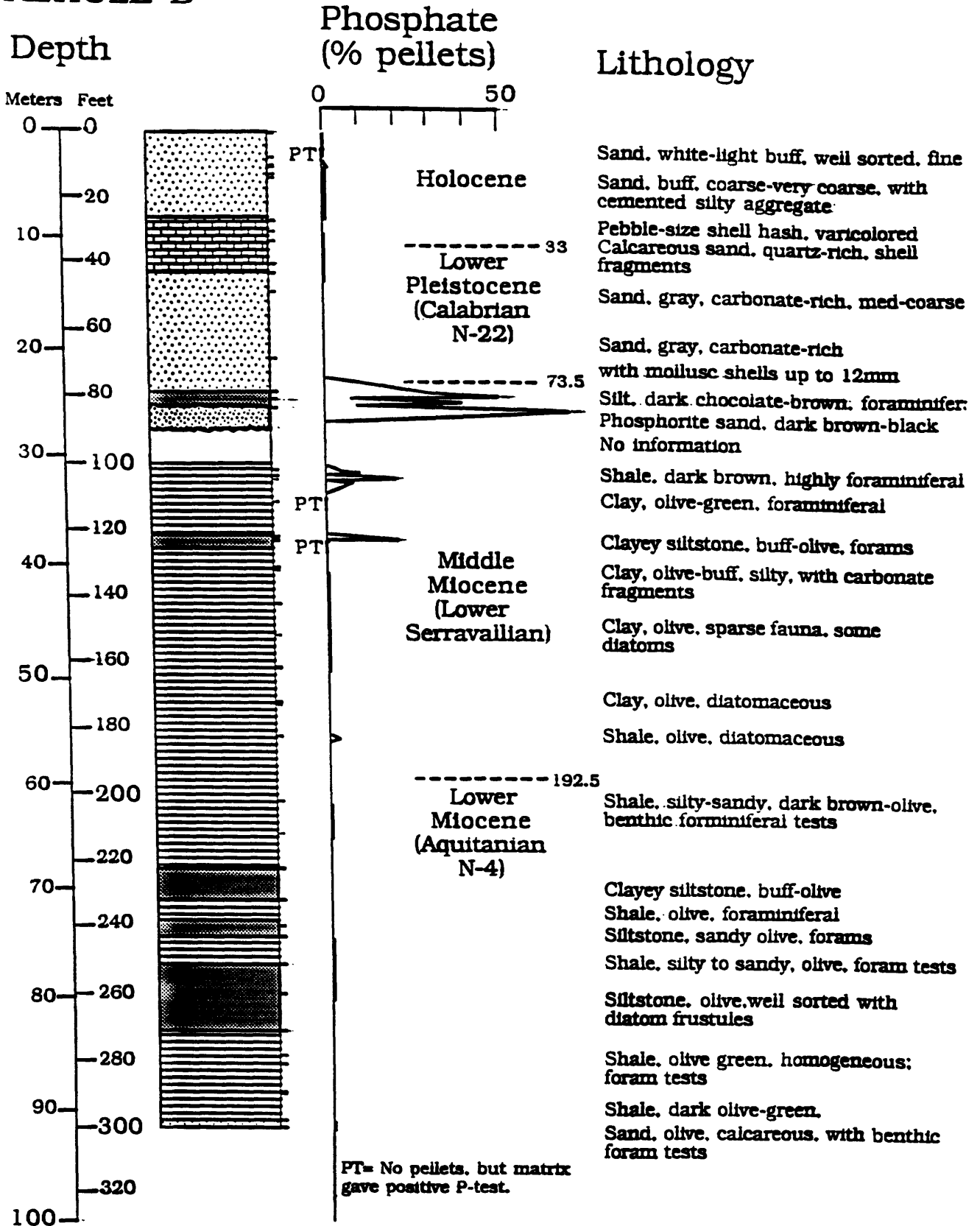


Figure III-3. Lithologic log for Tacts Borehole D. Ticks and bars along the right side of the lithology column refer to location and extent of samples. Dots - sand; fine dots = silt; short dashed line = silty-clay; lines = clay or shale; brick pattern - carbonate. In stratigraphic column letters refer to standard paleontologic time zones. Phosphate concentrations are estimated volumetrically by methods described in text. Source data under "Lithology" given in core description, Table 1.

BOREHOLE D

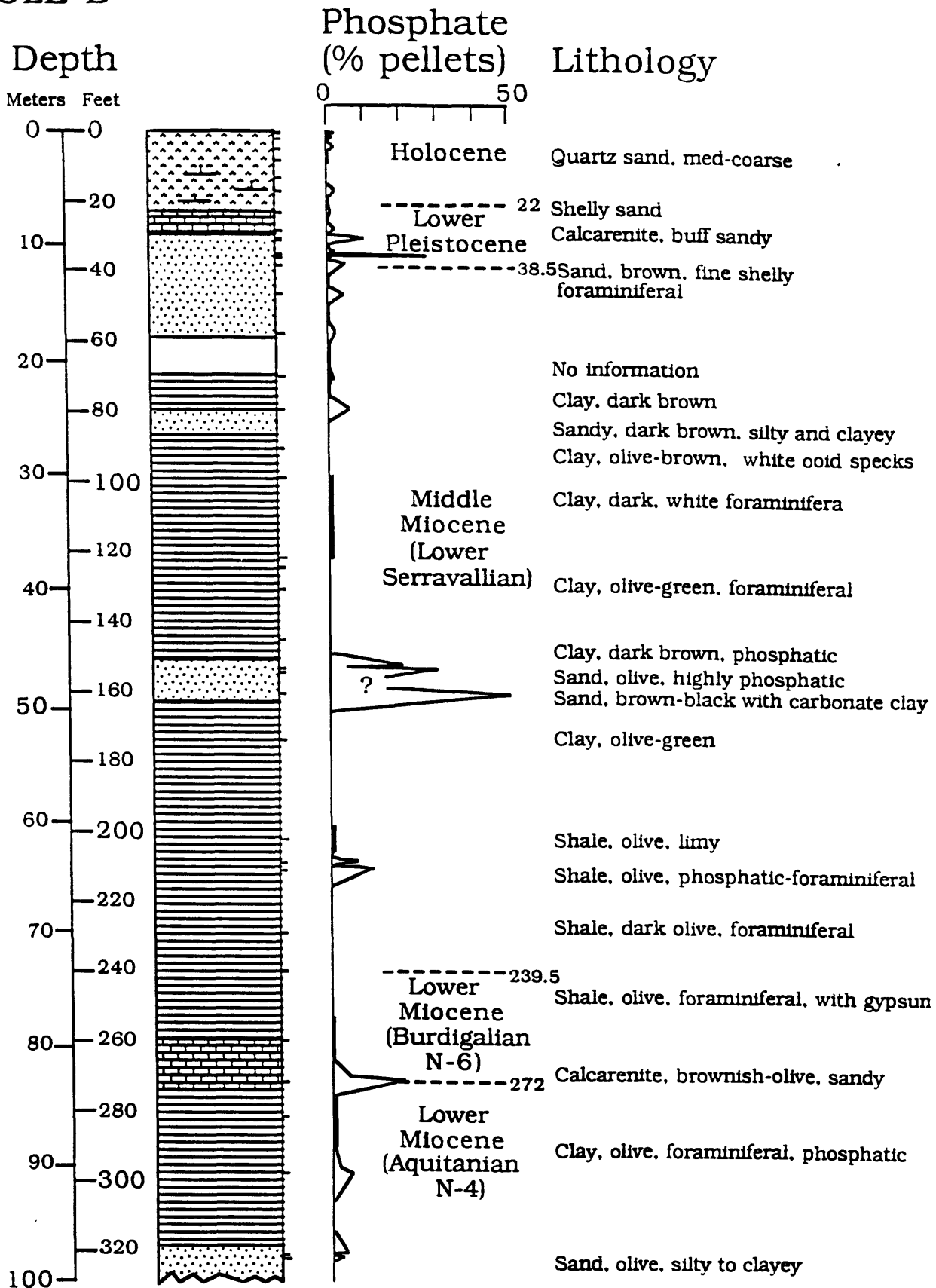
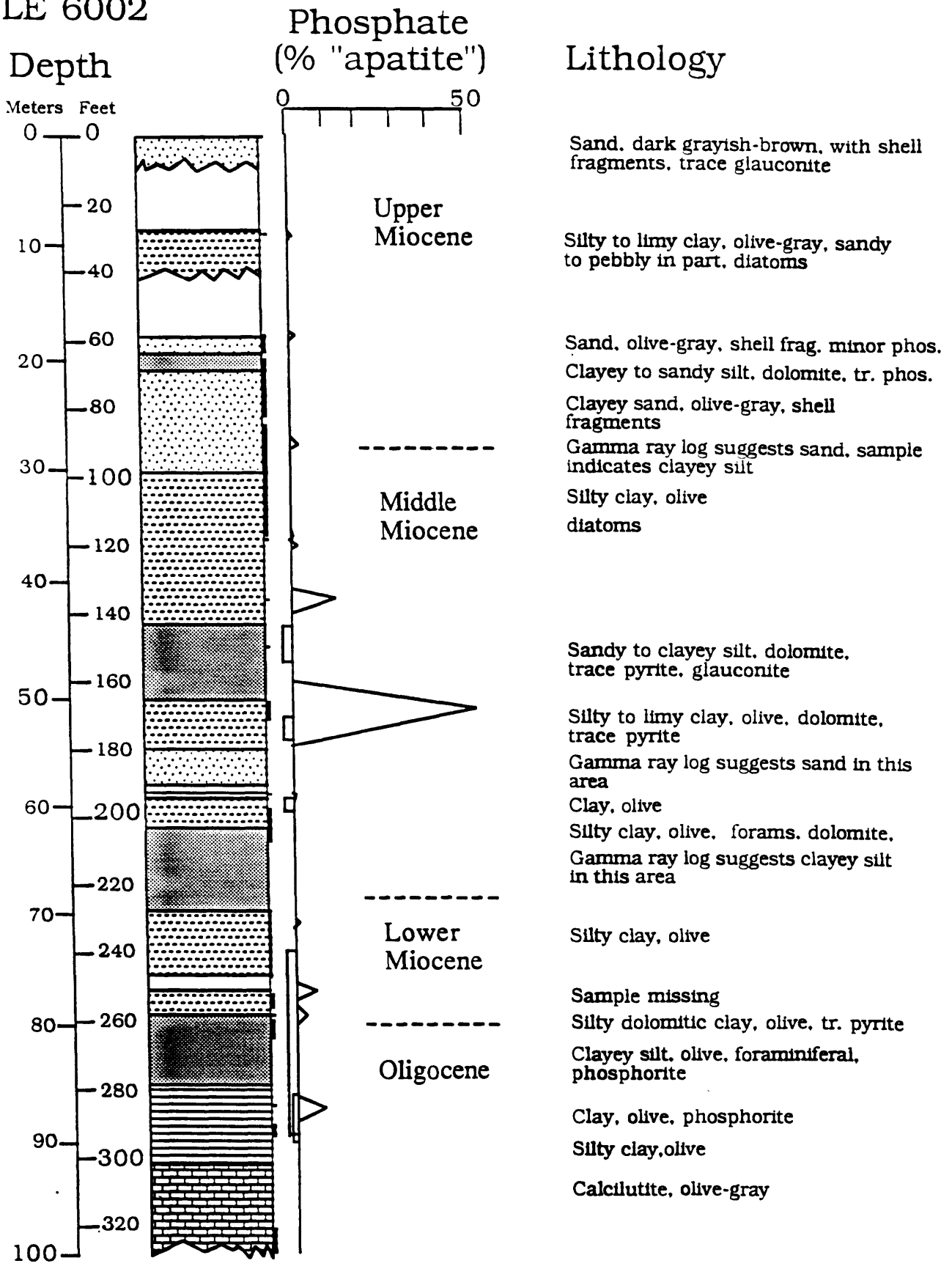


Figure III-4. Lithologic log for Tacts Borehole H. Ticks and bars along the right side of the lithology column refer to location and extent of samples. Dots - sand; fine dots = silt; short dashed line = silty-clay; lines = clay or shale; brick pattern - carbonate. In stratigraphic column letters refer to standard paleontologic time zones. Phosphate concentrations are estimated volumetrically by methods described in text. Source data under "Lithology" given in core description, Table 1.

Figure III-5. Lithologic log for AMCOR Hole 6002. Ticks and bars along the right side of the lithology column refer to location and extent of samples. Dots - sand; fine dots = silt; short dashed line = silty-clay; lines = clay or shale; brick pattern - carbonate. In stratigraphic column letters refer to standard paleontologic time zones. Phosphate concentrations are estimated volumetrically by methods described in text. Source data under "Lithology" given in core description, Table 1. "Apatite" is computed as shown in VI from chemical P_2O_5 values and is comparable to the "pellets" described visually for TACTS Boreholes B, D, and H. The source data for "Lithology" include Table 4, plus Schlumberger gamma ray neutron log. For other explanations see Fig. III-2.

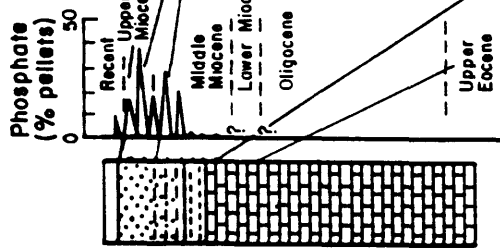
HOLE 6002



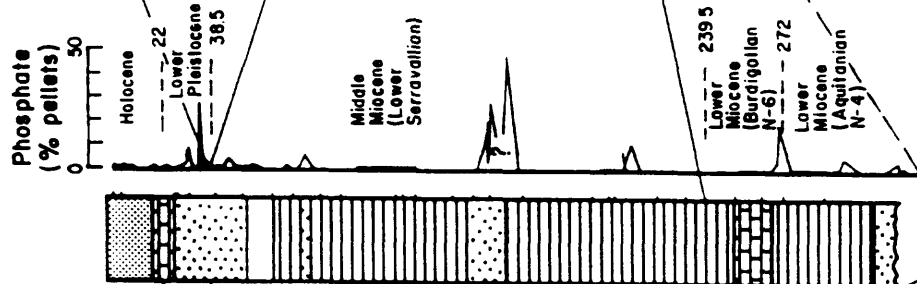
Zone of enhanced phosphorite according to the gamma ray log.

Figure III-6. Comparison of stratigraphic borehole profiles southeast from Savannah Light well. See location map, Fig. II-1 and lithological logs (Figs. III-1, and III-3 to III-5). All depths are sub-sea floor.

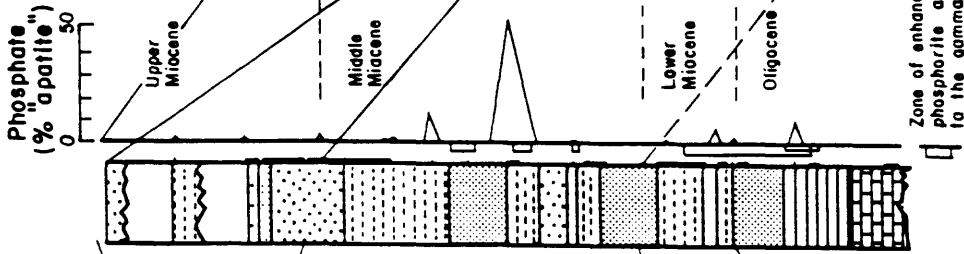
ICGT|SAVANNAH LIGHT



BOREHOLE D



HOLE 6002



BOREHOLE H

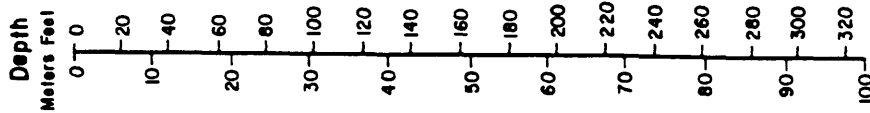
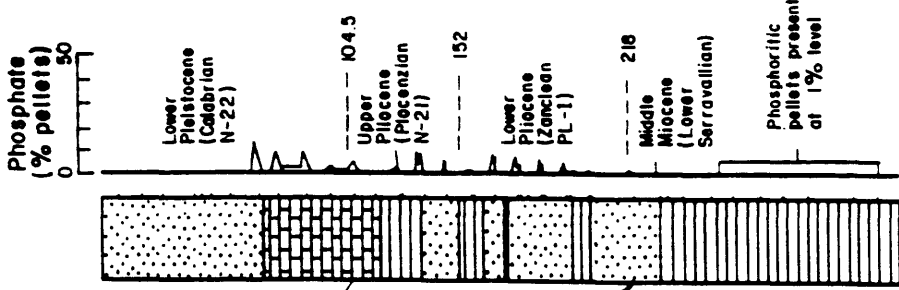
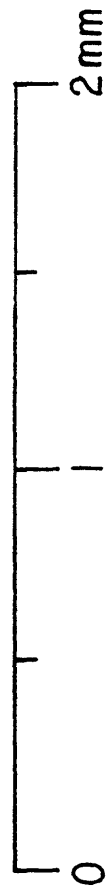
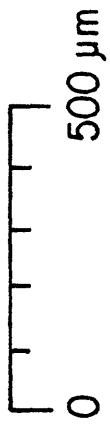
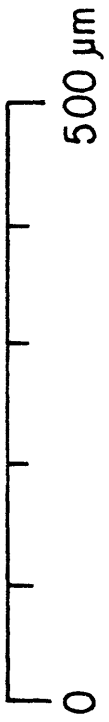


Figure III-7. Microphotograph of phosphorite-rich sediment, B81.5. Darker ovoid grains are phosphorite; white ones are mainly carbonate. Volumetric pellet estimate exceeds 60%.



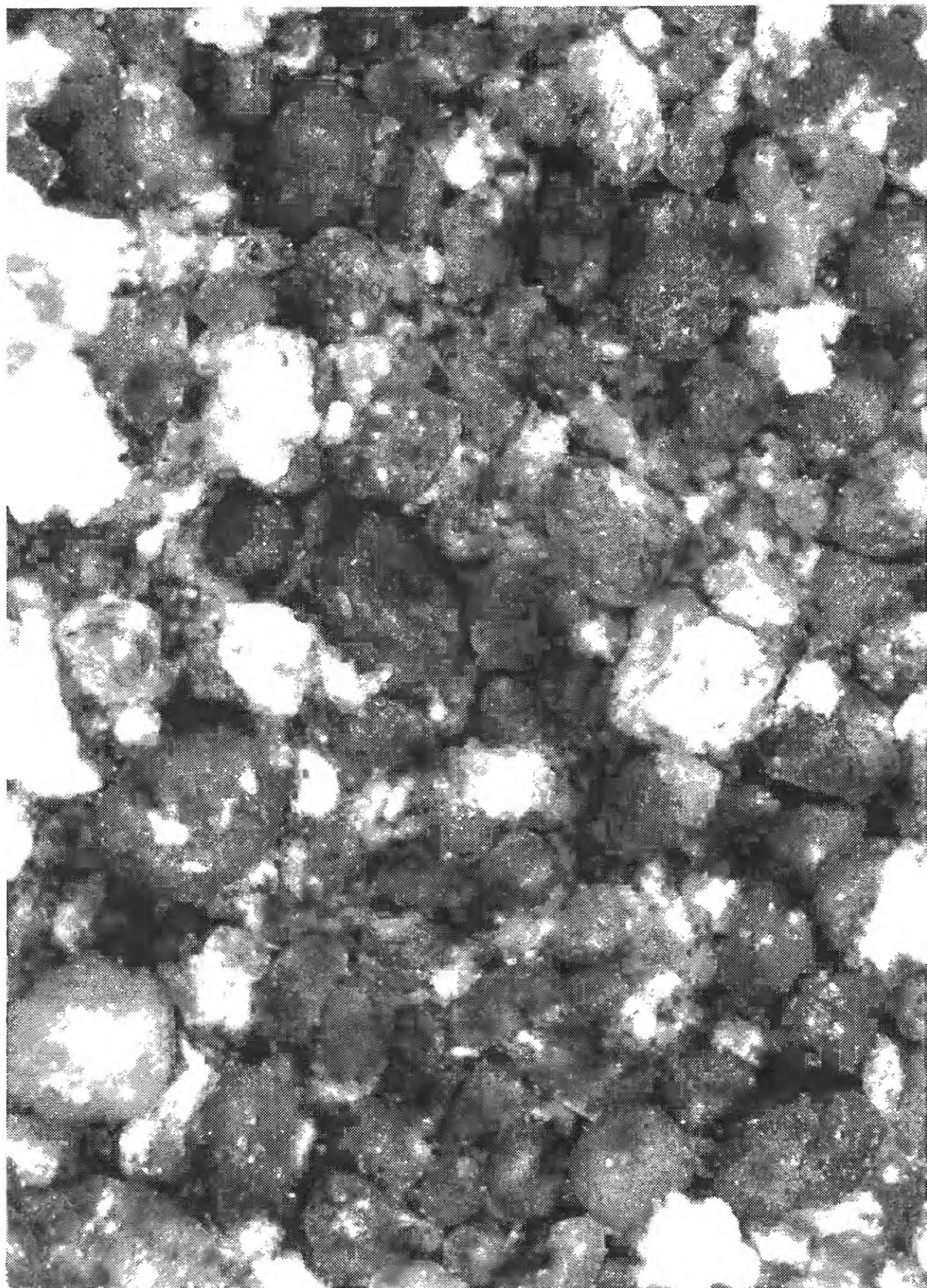


Table III-1. Lithologic description for TACTS Borehole B. Sample color refers to original sample observed by eye. Other description is by binocular microscope with assistance of 10% HCl, and qualitative molybdate test for phosphate. Textures are based on the Wentworth scale (very coarse 1-2, coarse .5-1, medium .25-.5, fine .124-.25, very fine .0625-.124, silt 1/16-1/256, clay <1/256mm). No effort was made to distinguish dolomite from other carbonate. Phosphate abundance estimated under microscope visually as discussed in text.

USGS Sample ID	Feet	Description
B0.2	0.5	Sand, white, poorly sorted, coarse to pebbles >10mm. Some coarse carbonate debris with scarce phosphorite pellets. Phosphorite pellets are black, polished and large, 0.5-0.7mm
B2.4	7.8	Sand, white-light buff, well-sorted, fine, liberally sprinkled with intense black particles having an irregular rough outline, generally non-phosphatic, but sample as a whole gives test for small amount of phosphate admixture. Very little sample remains
B3.0	10.0	Sand, buff, very poorly sorted, very coarse to fine with clasts of sand cemented and filled with gray-olive clay and silt. Phosphorite grains ~ 1.0% mostly normal pellet size (.2-.3mm) plus a few large, rounded impure grains to 0.7mm
B3.1	10.0C	As above without clay clasts
B3.2	10.5	As above, with rusty (secondarily altered), somewhat finer-grained. <=1% phosphorite, dark black-greenish; large brownish angular grains often do not test positively for P; large pectin shell fragment
B4.1	13.5	Sand, buff, coarse-very coarse with cemented silty-carbonate containing grains; these contain black oval grains about .5mm, phosphatic in part
B5.0	16.5	As above
B7.9	26.0	Rubbly pebble-sized shell hash, varicolored, highly cemented in bottom of jar. Colors range from white to buff, orange to deep red-brown-gray black; dark gray-black lumps seem to have much dispersed organic matter and give off petroleum smell on application of acid; no phosphate. Cementation has taken place post sampling
B9.1	30.0	Sandy shell hash with rounded carbonate concretionary pellets, .5-5mm, with much fine carbonate. Rounded black grains .5-1.5mm contain fine silt-size black particulate matter, partly phosphatic. Remaining sample cemented in bottom of jar
B10.0	33.0	Carbonate sand, quartz-rich; quartz ranges from medium-coarse whereas carbonate ranges from much larger shell fragments and

cemented grains to finer material. Many dark gray-black particles but most are non-phosphatic; phosphorite pellets (scarce) are round and shiny

- B12.2 40.0 Carbonate sand, orange-stained from corrosion of steel fragment; few round black phosphorite pellets and large piece of razor clam-like shell with outer honeycomb framework exposed by corrosion
- B12.8 42.0 Sand, gray shelly, coarse; pelecypod shell bored by gastropod, gray pepper & salt rounded fragments, 1-1.5mm, much very fine carbonate < 1mm-30um; little visible phosphorite, but sample as a whole shows phosphate test
- B14.6 48.0 Sand, gray, carbonate rich, medium-coarse with white weathered mollusc shell fragments and black carbonate grains, non-phosphatic.
- B20.9 68.5 As above, with mollusc shells to 12mm filled with cemented sandy carbonate mudstone mold, hard, speckled with darker carbonate fragments. Does not readily crumble apart as with superficial post-sampling cementation
- B24.6 79.0C Silt, dark chocolate-brown, well sorted, and foraminiferal with many tests mere residual fragments of test that has been largely dissolved away; highly phosphatic, 30-50%
- B24.7 81.0C Silt, clayey to fine-sandy, dark brown-chocolate with abundant phosphorite pellets making up nearly all sand-sized material, forams (planktonic) abundant; phosphorite 20-40%
- B24.8 81.5 Phosphorite sand, dark brown-black, .2-.3mm, slightly silty-clayey but these fractions are also dark with less frequent quartz sand grains and very rare forams. Phosphorite 60-70%, but only about 10g. sample left
- B30.6 100.5 Shale, dark-brown, highly foraminiferal, phosphatic, organic-rich, petroleum smell on applying acid; under high magnification shell matrix itself has a spherulitic appearance as though spherulites were molds of planktonic foraminifera. Pelletal material makes up 5-10% of sample
- B31.1 102.0 Silty clay, buff with darker layer characterized by admixture of typical phosphorite pellets, highly foraminiferal, 15-20% phosphorite pellets
- B31.1 102.0 Silty clay, olive, with sand-sized pellets (5-8%) and sparse carbonate tests
- B34.0 111.5 Clay, olive-green, foraminiferal; no pellets visible but clay matrix is phosphatic
- B37.2 122.0 Silty to sandy clay, olive, with phosphate pellets and some carbonate fragments; pellets are irregular in shape, 7-10%

- B37.3 122.5 Clayey siltstone, buff-olive, poorly consolidated with sand size white carbonate consisting in part of pellet size forams, largely mixed in origin. Few pellets are visible but matrix gives phosphate test
- B37.5 123.0 Clay, olive-green, few obvious microfossils and no pellets but matrix is slightly phosphatic
- B40.1 131.5 Clay, olive-buff, silty with abundant carbonate fragments
- B40.4 132.5 Clay, olive well-consolidated with many discoid diatom frustules, about .25mm; tend to disappear after acid treatment; pellets <1%
- B43.3 142.0 Clay, olive. sparse fauna, some diatoms, very sparse pellets but matrix yields positive P-test
- B46.3 152.0 As above
- B49.2 161.5 As above, slight gasoline smell on application of 10% HCl
- B49.5 162.5 As above, slightly silty
- B52.4 172.0 Clay, olive, diatomaceous
- B52.6 172.5 As above, dried sample shattered by gypsum growth
- B52.8 173.0 As above, scarce brownish particles
- B55.8 183.0 Shale, diatomaceous, olive, intercalated with shale having about 3% pellets; much gypsum. Carbonate tests can be observed to be replaced and filagreed by gypsum
- B61.6 202.0 Shale, silty-sandy, dark brown-olive phosphatic with pellets as well as many benthic foraminiferal tests
- B64.6 212.0 Shale, light olive, very sandy with carbonate microfossils; few pellets but matrix gives test
- B67.8 222.5 Clayey siltstone, buff-olive, white speckled with frosted carbonate tests; no pellets but gypsum growth
- B70.6 231.5 Shale, olive-white speckled with high foraminiferal content
- B73.2 240.0 Siltstone, sandy olive, speckled with white foram tests, some large Uvigerina-like specimens. No phosphate
- B73.8 242.0 Shale, silty to sandy, olive with white mixed foram and micromollusc(?) fauna; very small, scarce phosphorite pellets
- B76.5 251.0 Siltstone, clayey to sandy, olive, with abundant benthic foram tests and scattered pellets; rock disaggregates to rounded buff masses, partly phosphatic, that have similar size and shape as some benthic forams, to 1.2mm - protophosphorite?

- B79.4 260.0 Siltstone, olive, well sorted with diatom frustules and occasional phosphorite pellets
- B82.6 271.0 Shale, olive drag, silty-sandy with white sprinkles of benthic forams and ostracods(?)
- B85.0 279.0 Shale, olive-green homogeneous; foram tests not visible to the naked eye, but appear under microscope
- B85.6 281.0 Shale, sticky clayey, olive-green sparse fauna
- B88.2 289.5 Shale, olive-green, abundant foram tests but many have been converted to filagrees of gypsum
- B88.4 290.0 Shale, dark olive-green, gritty with abundant corroded and friable foram and microfossil tests. This specimen underwent considerable drying
- B91.1 299.0 Sand, olive calcareous with near micrococquina of benthic forams, 1% phosphorite pellets
- B91.4 300.0 Sand, olive-buff, fine-silty with white specklings of benthic foram tests and sparse phosphorite. Gasoline smell upon applying acid; dissolution of benthic foraminifera tests reveals many tiny pellets in chambers

Table III-2. Lithologic description for TACTS Borehole D. Other notes as in Table III-1.

USGS Sample ID	Feet	Description
D0.3	1.0	Quartz sand, white, clean, subrounded, medium to coarse with 10% carbonate fragments and <3% brown-black phosphorite grains
D0.7	2.4	Sand, gray-white, subangular to subrounded, medium-coarse, with light to dark gray carbonate fragments .5-4 mm , and 2% phosphorite grains, about .2 mm in diameter; quartz grains are mixed clear and frosted grains
D1.5	5.0	Quartz sand, shelly (gastropod fragments), poorly sorted, silty to coarse, 3% dark phosphorite grains; larger dark-green carbonate fragments are non-phosphatic and may be blackened shell
D2.7	9.0	Sand, very shelly (40-50%), fine to medium, mainly clear subrounded quartz; carbonate grains grade much finer: <1% phosphorite grains
D4.3	14.0	Two phases 1) sand, gray, shelly with highly frosted and recrystallized / leached gray carbonate grains; quartz is fine to medium (0.1-.5%) grains; 2) 2 balls of hard, shelly sandstone, similar texture as above; not certain whether 3 cm lumps are lithified in situ or after sampling
D5.2	17.0	Sand, buff, highly shelly, fine-medium, with white medium-coarse carbonate with a greater spread of textures (<.05-1.5 mm); some concretionary lumps 1-5 mm; 3% black phosphorite grains, .1-.3 mm
D6.9	22.5	Sandy calcarenite, buff-olive, partly cemented, fine-coarse (.2-.8 mm), 2% black-brown phosphorite grains, .2-.3 mm
D8.8	29.0	Calcarenite, buff-pale green, sandy in part, abundant benthic foraminifera, often partly altered and chalky in appearance; some cemented lumps, apparently natural, others questionable; carbonate size .2-3 mm, 3% dark brown-black phosphorite grains, angular
D9.4	31.0 31.5	Sand, brown shelly, phosphatic, fine-coarse, shell to 2 mm; both fresh and altered carbonate; much rusty-stained quartz(source of color), 6-10% phosphorite

- D10.7 35.0 Quartz sand, dark brown, fine, well-sorted, non-carbonatic with streaks of carbonate-rich white sand, .03-.3 (silty-fine sand), 1-3% phosphorite pellets
- D10.8 35.5 Sand, brown, highly phosphatic, shelly fine to coarse, many foram tests with adhering internal cemented molds; a few phosphate grains reach .4-.5 mm, unlike most pellets that maintain a consistent .2-.3 mm size
- D11.6 38.0 Iron-encrusted and cemented sandstone, brown, with softer partly unconsolidated material inside; rusty to dark-brown clayey layer; mollusk and foram fragments, microgastropods and bryozoa also; few phosphorite pellets
- D11.7 38.5 Sand, intense dark-brown, silty to fine, with occasional 1 mm quartz grain; 5% phosphorite made up of fine pellets .06-.1 mm
- D14.2 46.5 As above
- D17.8 58.5 As above, 3% larger phosphorite pellets, .1 mm
- D21.3 70.0 Clay, dark-brown with sprinkling of phosphorite (1% in .1-.2 mm pellets)
- D24.4 80.0 Sandy, very dark-brown, silty with clay admixture and occasional larger grains; sprinkling of foraminiferal tests; 6% phosphorite
- D27.6 90.5 Clay, olive-brown with ooid-like specks, possibly planktonic globigerinids
- D30.5 100.0 Clay, very dark with sprinkles of white planktonic? foraminifera and phosphorite; clay itself is phosphatic
- D36.9 121.0 Clay, olive green, silty with up to 25% well-preserved foraminifera, some with phosphorite grains inside; some may have lodged there mechanically but primary grains are not excluded
- D37.5 123.0 Clay, olive-green, highly foraminiferal, no visible phosphorite
- D39.9 131.0 Clay, olive-green, foraminiferal
- D44.2 145.0 Clay, olive, foraminiferal
- D46.9 154.0 Clay, dark-brown, phosphatic, 20% gray phosphorite particles make up the principal coarse matter, followed by white foram debris
- D47.1 154.5 Sand, olive, highly phosphatic, (25-30%) with sprinkling of foraminifera
- D49.1 161.0 Sand, intense brown-black phosphatic with carbonate and clay admixtures; petroleum smell on HCl application; samples may contain up to 50% phosphorite if majority of light brown grains are phosphorite (random samples tested positively)

- D53.0 174.0 Clay, olive-green
- D61.7 202.5 Shale, olive, limy (dolomitic?) (decrepitates with the application of 10% HCl); sparse phosphatic fragments and pellets
- D63.9 209.5 Shale, olive phosphatic-foraminiferal, 3-8% phosphorite pellets, standard .1-.3 mm size, carbonate plates and fragments 0.5-1.3 mm
- D64.3 211.0 Shale, olive phosphatic with 3-5% carbonate fragments, 0.05-2 mm, including both benthic and planktonic foraminifera. Petroliferous odor on applying acid; 8-12% phosphorite
- D70.0 229.5 Shale, dark olive foraminiferal, non-phosphatic
- D3.3 240.5 Shale, olive foraminiferal with many multifaceted crystalline balls of gypsum, .3-.8 mm, a few with crossed flat crystals (.5 mm) not primary, probably caused by interaction of oxidized pyrite sulfur with carbonate; dried cores often have a rubble of shale fragments created by the expansion of the gypsum
- D79.4 260.5 Calcarenite, light olive sandy, highly foraminiferal, with sprinkling of phosphate pellets; sand is <1 to 4 mm; petroleum smell released on acid treatment
- D82.9 272.0 Calcarenite, brownish olive, fine sandy, foraminiferal, phosphatic with much light brown irregular phosphate in the form of coatings up to 1.5 mm and irregularly shaped pieces; phosphorite 5-20%
- D85.8 281.5 Clay, olive, silty foraminiferal with fine phosphorite shown by chemical test (grains rare); 0.1 mm glistening gypsum crystals due to storage of core
- D91.0 298.5 Clay, olive, foraminiferal, phosphatic with larger gray black 4 mm 1 rounded nodules, hard, some with hollow center; some silt and occasionally sand-gray. 3-6% phosphorite pellets
- D98.3 322.5 Sand, olive, silty to clayey phosphatic; includes both standard .1-.2% brownish-black pellets, irregular larger gray-black rounded grains, 0.5-2 mm, and irregular brownish recrystallized phosphorite; total average 5%
- D98.5 323.0 As above, much gypsum, less phosphorite but large phosphatic grains to 3 mm still present

Table III-3. Lithologic description for Tacts Borehole H. Other notes as in Table III-1.

USGS Sample ID	Feet	Description
H1.7	5.5	Sand, grayish, poorly sorted, <1% phosphorite, scattered shell fragments
H4.7	15.5	Sand, gray and white, poorly sorted, medium to very coarse, no phosphorites
H7.5	24.5	Pebbles of lithified carbonate, gray-black with pseudo-conchoidal fracture and brownish interstitial matter .5-1.5 cm along with white quartz sand, slightly limey with 2mm ooids on quartz grains; very smooth black grains not phosphorite
H11.1	36.5	Sand, white-gray, poorly sorted, fine to very coarse, <1% phosphorite, shell fragments, various sized ooids on quartz grains
H12.2	40.1	Pebbles and sand, gray and white, poorly sorted, fine to very coarse, <1% phosphorite, shell fragments, various sized carbonate ooids on quartz grains
H13.6	44.5	Sand, carbonate cemented aggregate (probably cemented after sampling), light gray, fairly well sorted, medium grain, cemented aggregate 8 x 10mm, <1% phosphorite, few shell fragments
H15.8	52.0	Clayey sand, light gray, poorly sorted, very fine to coarse ~2% phosphorite, shell fragments throughout
H18.9	62.0	Sandy clayey carbonate, light gray/brown, poorly sorted, fine to coarse, 6-12% phosphorite
H22.0	72.0	Calcareous sand, buff, poorly sorted, very fine to coarse, with minor admixture of quartz; carbonate is altered, milky looking, but benthic organisms are still visible, 6-8% phosphorite pellets. Two types of pellets, brown are smaller in size, gray-black range in size up to 2mm
H25.6	84.0	Calcareous sand, light gray/brown, poorly sorted, very fine to coarse, 6-8% phosphorite
H28.7	94.0	Calcareous sand, buff, very (quartz) sandy, medium, highly foraminiferal (benthic), 2% phosphorite pellets

H31.9 104.5 Calcareous sand, buff-olive, medium coarse with large carbonate grains, including benthic forams, heavily frosted chalky in appearance, large (fine to medium sand sized) phosphorite pellets, 4%

H34.4 113.0 Calcareous sand, buff, fairly well sorted, fine to very fine, <1% phosphorite, shell fragments

H37.8 124.0C Calcareous sand, medium to coarse (.2-.7mm), with much foram debris plus cemented carbonate ooze in rounded, ooid-like aggregates; sparse phosphorite pellets, <1%

H40.5 133.0C Calcareous sand, buff, chalky cemented, with 8% phosphorite pellets

H40.7 133.5C As above, but fine grained, except for shell fragments, <1% phosphorite

H40.9 134.0 Silty clay, light brown, with very fine sand; sediment had pasty texture and clumps of denser material of same color, forams, 5% phosphorites

H43.3 142.0C Sand, buff-olive, fine with calcareous admixture; 1-2% phosphorite pellets

H43.4 142.5C Mainly sand with minor clay, light gray/brown, well sorted, fine grained 3-4% phosphorite, several white clay clasts of different shapes and sizes, forams

H43.6 143.0 Sandy carbonate, olive green, fairly well sorted, fine to medium grain, 3-5% phosphorite, forams

H46.3 152.0 Sand, olive, well sorted, fine, 1% phosphorite

H46.5 152.5 Sand dark clay admixture, olive/brown, well sorted, fine grained, dense clumps of clay and sand, 1-2% phosphorite, occasional carbonate shell fragments

H46.6 153.0 Sandy clay, dark brown, fairly well sorted, very fine to fine. 1-2% phosphorites, some shell fragments

H49.4 162.0 Sand, dark-olive, fine to very fine, well sorted with sparse carbonate shell fragments (.2-.4mm) and phosphorite pellets 3-4%

H49.5 162.5C Sand, dark olive, well sorted, fine to very fine with sparse carbonate(shell) fragments(.2-.4mm) and phosphorite pellets 3-4%

H49.7 163.0 Sandy clay, dark olive/brown, moist, well sorted, fine to very fine, 4-6% phosphorites, sparse forams, shell fragments

H52.1 171.0 Sandy clay, dark olive, well sorted, very fine, 4-6% phosphorite with some carbonate

H52.4 172.0 Sand, dark brown, fine, well sorted, sparse carbonate and

		phosphorite 2-3%
H55.2	181.0	As above, silty with ~ 5% phosphorites
H55.4	182.0	Sand, dark brown, well sorted, fine grain, sparse carbonate and phosphate 4-5%
H58.2	191.0	Sand, dark brown, 2% dark, well sorted, fine, 2-3% phosphorite pellets
H58.4	191.5C	Silty sandy clay, dark olive, well sorted, fine grain, 2-4% phosphorite, sparse carbonates
H58.5	192.0	As above, 4-5% phosphorites
H58.7	192.5	As above, 2-3% phosphorites
H59.0	193.5	As above, 1% phosphorites
H61.0	200.0C	Sand, dark olive-green, well sorted, fine to very fine, speckled with dark phosphorite pellets of corresponding size (<1%); streaks of dark brown-gray clay, .5-1mm wide
H61.1	200.5C	Sand and clay, dark olive, well sorted, fine to very fine, <1% phosphorite
H61.3	201.0	As above, 1% phosphorite pellets
H66.8	219.0	Sand, light brown, fairly well sorted, fine grained, 1-2% phosphorite of different sizes
H69.8	229.0C	Sand, dark brown, white buff clay clasts, fairly well sorted, fine grained, various sized and shaped phosphorite pellets 2-4%
H70.0	229.5C	Sand, dark brown-olive, micaceous looking in part, with buff clay clasts, 5-10 mm, and variably shaped and sized phosphorite pellets, 2-3%, clay clasts have sharp edged irregular boundaries, clay has slightly phosphatic reaction
H70.4	231.0C	Sandy clay, light olive, fine grained, large percentage carbonate microfossils, no phosphorite pellets, however, sample produces a positive P test
H70.6	231.5C	As above
H72.9	239.0C	As above, with very small phosphorite grains <1%
H73.0	239.5C	As above, <1% phosphorite, many of the microfossils contained within their tests micropellets of phosphorite. Some of the microfossils had chambers that were full of the pellets while others had very few pellets
H75.9	249.0	Clay, light olive green, containing mainly microfossils, no apparent phosphorite, sample gives a positive P test, emits a

petroleum smell when acid is added

H78.0	259.0C	Clay with very little fine grained sand, olive green, sample is full of microfossils similar to those stated above, sample gives positive P test, although little phosphorite may be seen
H82.0	269.0C	As above
H82.1	269.5	As above
H85.0	279.0C	As above
H85.2	279.5C	As above
H88.1	289.0C	As above, with some planktonic forams included.
H88.2	289.5	As above
H94.2	309.0C	As above, contains some glauconite pellets throughout
H94.2	309.0	As above, contains few rather large phosphorite pellets
H97.2	319.0	As above

Table III-4. Lithologic description for AMCOR Hole 6002. The data cited here are taken from "Visual Core Descriptions" of the Atlantic Margin Coring Project, 1976, from "Smear Slide Data" and from later laboratory measurements (Poppe, 1981). Percentage numbers before the phase refer to visual or x-ray diffractions estimation. Percentages after the phase refer to chemical determinations. The depths are nominal, taken mainly from Appendix I in Poppe (1981). The decimal numbers are reported for consistency and to indicate approximate distance between samples only.

Core	Sec.	Depth		Description
		Meters	Feet	
1	1	.1	.3	Sand, dark grayish brown, quartz, shell fragments, trace glauconite, possible trace apatite; CaCO ₃ 9.1%, 7.3%, P ₂ O ₅ .13%, .18%
2	1	8.3	27.2	Silty to limy clay, olive gray, sandy, pebbly, trace dolomite, possible trace apatite, abundant diatoms, CaCO ₃ 18.8%, P ₂ O ₅ .99%
3	1	17.8	58.4	Sand, olive gray, phosphate and shell fragments, P ₂ O ₅ 1.85%
3	2	19.5	64.0	Clayey to sandy silt, 28% dolomite, 1% pyrite, 1% apatite
3	3	20.6	67.6	Silty clay, olive gray
		21.2	69.5	Clayey sand, olive gray, with shell fragments
3	4	22.2	72.8	Same as above
3	5	23.	78.4	Clayey sand, olive, shell fragments
		24.7	81.0	Clay, olive
		24.	81.3	Clayey sand, olive, shell fragments
3	6	26.1	85.6	Clayey sand, olive, shell fragments, coarse, massive bedded, well mixed
		26.4	86.6	Silty to clayey sand, olive, fine, apatite pellets?
		27.2	89.2	As above, bioturbated?, not well mixed
4	1	27.5	90.2	Silty clay, olive, P ₂ O ₅ 2.34%
4	2	28.2	92.5	Clayey silt, minor sand, olive, 10% dolomite, 1% pyrite, 15% diatoms, sponge spicules
4	3	30.5	100.0	Silty clay, olive

4	4	31.5	103.3	Silty clay, olive
4	5	32.	107.3	As above
4	6	35.5	116.4	Silty clay, olive, 30% diatoms, sponge spicules, and radiolarians; dolomite 22.2%, P ₂ O ₅ 1.50%
5	1	36.1	118.4	Silty clay, olive, P ₂ O ₅ .81%
		36.1	118.4	Clay,olive
6	1	41.2	135.1	Silty clay, olive, P ₂ O ₅ 1.57%, 7.04%, 1.57%
6	2	45.6	149.6	Sandy to clayey silt, trace pyrite, glauconite, 14% dolomite
7	1	50.6	166.0	Silty clay, olive
7	2	51.3	168.3	Silty clay, olive, no apatite, 26% dolomite, 2% pyriteCaCO ₃ 18.4%, P ₂ O ₅ 23.35%
8	1	59.4	194.8	Clay, olive, P ₂ O ₅ .99%
8	2	60.3	197.8	Silty clay, olive
8	3	61.8	202.7	Silty clay, olive, nannofossils, trace pyrite, forams, dolomite, CaCO ₃ 18.3%
9	1	69.3	227.3	Silty clay, olive
9	2	70.7	231.9	Silty clay, olive, P ₂ O ₅ 1.05%
9	3	72.2	236.8	Silty clay, olive
9	4	73.7	241.7	Silty clay, olive
9	5	75.2	246.7	Sample missing
9	6	76.7	251.6	Silty dolomitic clay, olive, trace pyrite, forams, nannofossils, CaCO ₃ 36.0%, P ₂ O ₅ 3.37%
10	1	79.0	259.1	Silty clay, olive
10	2	79.2	259.8	Clayey silt, olive, trace pyrite, dolomite, 10% forams, calc. nannos, CaCO ₃ 36.8%, 38.4%, P ₂ O ₅ 2.15%
11	1	86.6	284.0	Clay, olive, P ₂ O ₅ 5.06%
11	2	88.3	289.6	Silty clay, minor sand, olive

12	1	97.9	321.1	Calcilutite, olive gray, P ₂ O ₅ .38%
12	2	98.2	322.1	Calcilutite, olive gray
12	3	99.7	327.0	Calcilutite, olive gray
13	1	107.4	352.3	Silty carbonate, olive gray, P ₂ O ₅ .25%
14	1	117.1	384.1	Clayey carbonate, lt olive gray
14	2			Contained only water
14	3			As above
14	4			As above
14	5	123.7	405.7	Silty clay, nannofossil rich, light olive gray, trace glauconite, pyrite, 15% zeolite
14	6	124.0	406.7	Silty clay, carbonate rich, light olive gray, trace glauconite, pyrite, dolomite, diatoms, possible trace apatite
15	1	126.6	415.2	Carbonate, light olive gray, P ₂ O ₅ .31
15	2	128.	419.8	Clayey to silty carbonate, light olive gray, trace pyrite, 5% zeolite, CaCO ₃ 70.7%, 72.7%
15	3	129.0	423.1	Carbonate, light olive gray
15	4	129.8	425.7	Silty carbonate, light olive gray,
16	1	136.0	446.1	Silty carbonate, light olive gray, large mollusk fragments scattered throughout
16	2	137.1	449.7	Silty carbonate, light olive gray, slight phosphate, limestone, light olive gray, some shells, phosphate P ₂ O ₅ .60%, .68%.
		137.5	451.0	Clayey carbonate sand, olive gray, phosphatic, shells
16	3	139.3	456.9	Limestone, light olive gray, fossiliferous
		139.4	457.2	Silty carbonate, light olive gray P ₂ O ₅ .26%

17	1	146.1	479.2	Silty carbonate, light olive gray
17	2	147.2	482.8	Chalk, light olive gray, 5% zeolite, CaCO ₃ 86.7%, 87.0% light carbonate is probably recrystallized nannofossils
17	3	149.0	488.7	Silty clayey carbonate sand, light olive gray, scattered phosphatic grains, scattered large mollusk fragments, P ₂ O ₅ .59%, 1.83%
17	4	153.5	503.5	Sandy carbonate, light olive gray, phosphatic, large mollusk fragments scattered throughout
18	cc	164.3	538.9	Core catcher only, fine white sand and shells
19	1	164.4	539.2	Limestone, light olive gray, fine grained, P ₂ O ₅ .19%
19	2	165.4	542.5	Silty zeolitic carbonate sand, light gray, trace pyrite, CaCO ₃ 82.7%, 82.1%
19	3	170.7	559.9	Limestone, light gray, megafossils, phosphate?
19	4	172.	564.8	Limestone, clay, light gray, fossils present
20	1	174.4	572.0	Limestone, light olive gray
20	2	175.9	577.0	Calcareous limestone, light olive gray
20	3	177.0	580.6	Limestone, light olive gray, P ₂ O ₅ .15%
20	4	180.2	591.1	Clayey limestone, light gray
20	5	181.7	596.0	Clayey silty limetone, light gray
21	cc	192.6	631.7	Core catcher only, limestone
22	1	192.9	632.7	Slightly silty carbonate sand, light gray, trace dolomite, CaCO ₃ 92.7%, P ₂ O ₅ .15%, .14%
22	cc	197.0	646.2	Limestone, core catcher; no other information
23	1	202.6	664.5	Clayey limestone, light gray, fossils present

23	2	203.8	668.5	Silty carbonate sand, light gray, trace dolomite, glauconite, CaCO ₃ 88.8%, P ₂ O ₅ .16%
23	3	206.0	675.7	Clayey limestone, light gray
24	1	211.7	694.4	Silty carbonate sand, light gray, trace dolomite, zeolite, CaCO ₃ 90.9%, P ₂ O ₅ .17%, .25%
		212.7	697.7	Limestone, fossiliferous, light gray, scattered phosphate grains
25	cc	221.4	726.2	Core catcher only, hard white sandy limestone
26	cc	235.2	771.5	Core catcher only, recovered, limestone
27	cc	240.1	787.5	Core catcher only, hard white sandy limestone, P ₂ O ₅ .14%
28	1	249.9	819.7	Silty carbonate sand, light olive gray, trace glauconite, CaCO ₃ 86.4%
29	cc	263.8	865.3	Core catcher only, fossiliferous, clayey sand
30	cc	273.3	896.4	Core catcher only, hard limestone and fine sand
31	cc	282.7	927.3	Core catcher only, hard limestone fragments and fine sand
32	cc	287.6	943.3	Core catcher only, hard fine grains of white limestone
33	1	297.9	977.1	Zeolitic carbonate silt, light gray, CaCO ₃ 54.7%, P ₂ O ₅ .11%, .09%

IV Chemical analyses

By J.A. Commeau and F.T. Manheim

The chemical analyses clearly corroborate the visual estimations of phosphorite presence, indicating, on balance, higher concentrations than indicated by the latter method. As may be seen in Table IV-1 and Table IV-2, values as high as 21.6% P_2O_5 (47.2% BPL) are obtained at unconformities. Approximately 18 separate core samples yielded values having 10 volume % phosphorite pellets or more since sample coverage is estimated to make up only about 8%.

Differences in concentrations shown in Tables VII.1 and VII.2 are partly explained by the fact that the visual method of analysis estimates only pellets, whereas significant amounts of phosphate were observed in the fine matrix by qualitative chemical tests during the the microscopic analysis.

The microscopic and chemical samplings were taken from the cores or bottled samples without any attempt at homogenization. A large but unknown proportion of the variability is therefore due to inhomogeneous distribution of phosphate within the samples. Finally, the visual method of estimation is subject to considerably larger error than the chemical method, due largely to uncertainties in conversion of area estimates of randomly occurring pellets to volume. The two methods form excellent complements to each other, the visual observations being rapid enough to yield comprehensive sample coverage as well as information on pellet concentration, while the chemical analyses yield more precise data on total phosphate content, as well as information on other chemical constituents.

Work on more extensive chemical information, including trace elements, is continuing (J. Herring and F. Manheim).

The major element analyses of 20 samples of TACTS and comparative sediment materials have been performed by lithium borate fusion and X-ray fluorescence spectrometry in the Woods Hole laboratories of the U.S. Geological Survey. Ten of these are shown along with corresponding volumetric estimates of phosphorite pellet concentrations in Tables IV-1 and IV-2.

The elements and components needed to approach a sum of 100%, but which were not routinely analyzed in present data, include Na, Cl, and especially SO_3 associated with gypsum. A sample analysis of SO_3 was performed by direct powder analysis by X-ray fluorescence and yielded the value shown for sample B.8.1.5. The conversion formula used in the tables are indicated below.

$$\begin{aligned} CO_2^* &= 0.784 (CaO_{tot} - 1.567P_2O_5) \\ F^* &= 0.137P_2O_5 \\ BPL &= 2.185P_2O_5 \\ P2O5 &= 1.053V_f/[1.053V_f + (1-V_f)D_{sed}] \end{aligned}$$

where * refers to values computed from CaO and/or P_2O_5 , BPL refers to bone phosphate of lime, $Ca_3(P_2O_5)_2$, $P_2O_5 = P_2O_5$ % by weight computed from volumetric phosphorite (francolite) estimates, and D_{sed} = bulk density of non-phosphatic sediment in g/cm^3 . CaO_{tot} refers to total CaO in the sample, and $*CO_2$ refers to excess CO_2 associated with free carbonates (e.g. calcite or dolomite) but not CO_2 associated in the apatite lattice. The chemical relationships are based on pure carbonate fluorapatite (CFA) averages for North Carolina phosphorites (Van Kauwenbergh and McClellan, 1985).

One final set of data is mentioned here: the indications of a petroleum-like smell that were found at intervals throughout the cores when samples were treated with acid. These indications were particularly noted in the dark, organic-rich layers, often with significant amounts of phosphorite. They were not obtained in the post-Miocene layers, even those that contained phosphorite. There was no evidence of any contamination by diesel fuel or other artificial sources of hydrocarbon.

Jean Whelan and Marta Tarafa of the Woods Hole Oceanographic Institution kindly undertook pyrolysis analysis of samples from Hole B to determine if any migrated or other hydrocarbon was present. The results of the analyses showed pyrolysis values typical for immature sediments, without any evidence of migrated or generated petroleum. Pyrolysis C1-C3 values (methane-ethane-propane) within the Miocene strata indicate significant gas generating potential, especially within dark-brown, foraminiferal shales. The investigators found the pyrolysis curves to track lithology fairly well. The source of the odor remains unknown.

Table IV-1.

Chemical composition of sediment samples in weight percent. Sum includes all constituents to its left. * refers to values computed from CaO and P₂O₅. ** refers to SO₃ value of 6.7% estimated for powdered samples by X-ray fluorescence spectrometry. Loss on ignition (LOI) refers to ignition at 1000°C for 1 hours.

Sample #	SiO ₂	TiO ₂	Al ₂ O ₃	Fe ₂ O ₃	CaO	MgO	K ₂ O	P ₂ O ₅	LOI	SUM	H ₂ O-	CO ₂ *	F**
B79	21.6	0.14	1.7	0.65	28.9	6.6	0.53	11.0	22.8	93.9	1.4	9.5	1.5
B81.5	10.1	0.06	1.1	0.38	39.7	2.0	0.26	21.6	14.2	89.4**	1.1	5.5	3.0
B102	23.3	0.25	3.0	1.76	24.1	6.2	0.65	16.7	22.4	98.36	2.0	0	2.3
B111.5	29.9	0.23	2.3	1.76	18.6	4.5	0.57	6.7	22.9	87.46	1.9	6.7	0.9
B172	46.4	0.32	3.6	2.08	8.5	5.1	0.77	1.36	22.4	90.53	2.0	5.0	0.2
D35.5	53.4	0.36	3.7	1.38	12.8	<1.0	1.45	5.0	8.9	86.99	0.8	4.1	0.7
D154	17.7	0.10	1.6	0.91	34.3	1.4	0.52	15.2	17.1	88.83	1.4	8.8	2.1
D154.5	16.1	0.07	1.5	1.06	36.1	1.0	0.42	17.0	15.4	89.83	1.0	4.4	2.3
D272	38.1	0.25	2.4	0.72	24.0	<1.0	0.89	4.1	17.5	87.96	0.5	13.9	0.6
D62	31.4	0.01	0.4	0.47	30.6	<1.0	0.21	3.9	23.6	87.59	0.4	19.4	0.5

Table IV-2. Comparison of chemical and volumetric chemical equivalents based on different samples from common sediment horizons.

Sample #	Chemical analysis	Volumetric analyses			Mean Pellet Volume(%)
	(wt%) P ₂ O ₅ %	Mean%	Minimum%	Maximum%	
B79	11.0	14.1	10.5	17.6	33
B81.5	21.6	17.9	16.5	19.3	65
B102	16.7	8.2	7.0	9.4	50
B111.5	6.7	<1	-	<1	<1
B172	1.36	<1	-	<1	<1
B35.5	5.0	9.1	4.6	13.7	15
B154	15.2	9.1	-	-	45.6
B154.5	17.0	11.3	10.3	12.3	51
B272	4.1	6.4	2.6	6.4	12
B62	3.9	4.9	3.3	6.5	12

V Regional summary of the Geology of the Miocene of Georgia, and observations from the seismic-reflection profiles and the TACTS cores

By P. Popenoe, P. F. Huddlestun, and J. V. Henry

The continental shelf and slope off Georgia are covered with one of the most extensive networks of high-resolution, seismic-reflection surveys to be found on the Atlantic margin (Fig. V-1). The network of traverses were collected by the U.S. Geological Survey and by the University of Georgia under an environmental studies program conducted jointly by the USGS and the U.S. Bureau of Land Management (under functions later assumed by the Minerals Management Service). The studies program was initiated prior to OCS Lease Sales 43 and 56, when information was needed on the geologic hazards and constraints to petroleum exploration and development activities on the Outer Continental Shelf.

These data are now being used to estimate the heavy mineral and phosphorite potential of the southeastern continental shelf. Existing coverage is shown in Figs. V-1 and V-2.

In spite of the density of track lines, previous use of the data set has always been hampered by a lack of stratigraphic ties to core data with modern foraminiferal biostratigraphy. With the TACTS cores we now have a much better biostratigraphic and lithostratigraphic framework on which to base the seismic analyses.

Age dates from TACTS cores B, D, and H, combined with the seismic stratigraphic data, yield correlations that help predict the thickness and extent of the various Miocene units, their lithology, and environment of deposition, and the location and depth of the most phosphatic layers. The analyses of the cores in combination with the seismic data set forms much of the basis for the following discussion.

The Miocene sediments of southeastern Georgia record five major sea level rises across the continental shelf and into a low area that underlay eastern Georgia (the Waycross Basin and Gulf Trough of Figures V-3 and V-4). The high sea-level stands are separated by intervening sea-level falls that produced recognizable unconformities under the shelf. The major phosphorite enrichment zones occur along these unconformities and can be traced the seismic stratigraphic data. The following observations are preliminary and are based on only three of the eight TACTS boreholes, plus restudied sections of earlier boreholes.

Aquitanian (Early Miocene)

The first major sea-level rise was a continuation of a rise that began in the late Oligocene (Chattian), and continued with only a minor fall into the earliest Miocene (Aquitanian). During the late Oligocene, the continental shelf and a low area that constituted eastern and central Georgia were flooded by marine seas. During this flooding, the Suwannee Limestone was deposited across much of central Georgia and the more clastic Cooper Formation was deposited in eastern South Carolina. Following a slight fall of sea level at the close of the Oligocene, the rise continued and the Parachucla Formation of Georgia and Edisto Formation of South Carolina, both of Aquitanian age, were deposited in the seaway across southern and central Georgia.

Figure V-1. Tracklines of USGS high-resolution seismic reflection profiles across the continental shelf and slope off Georgia.

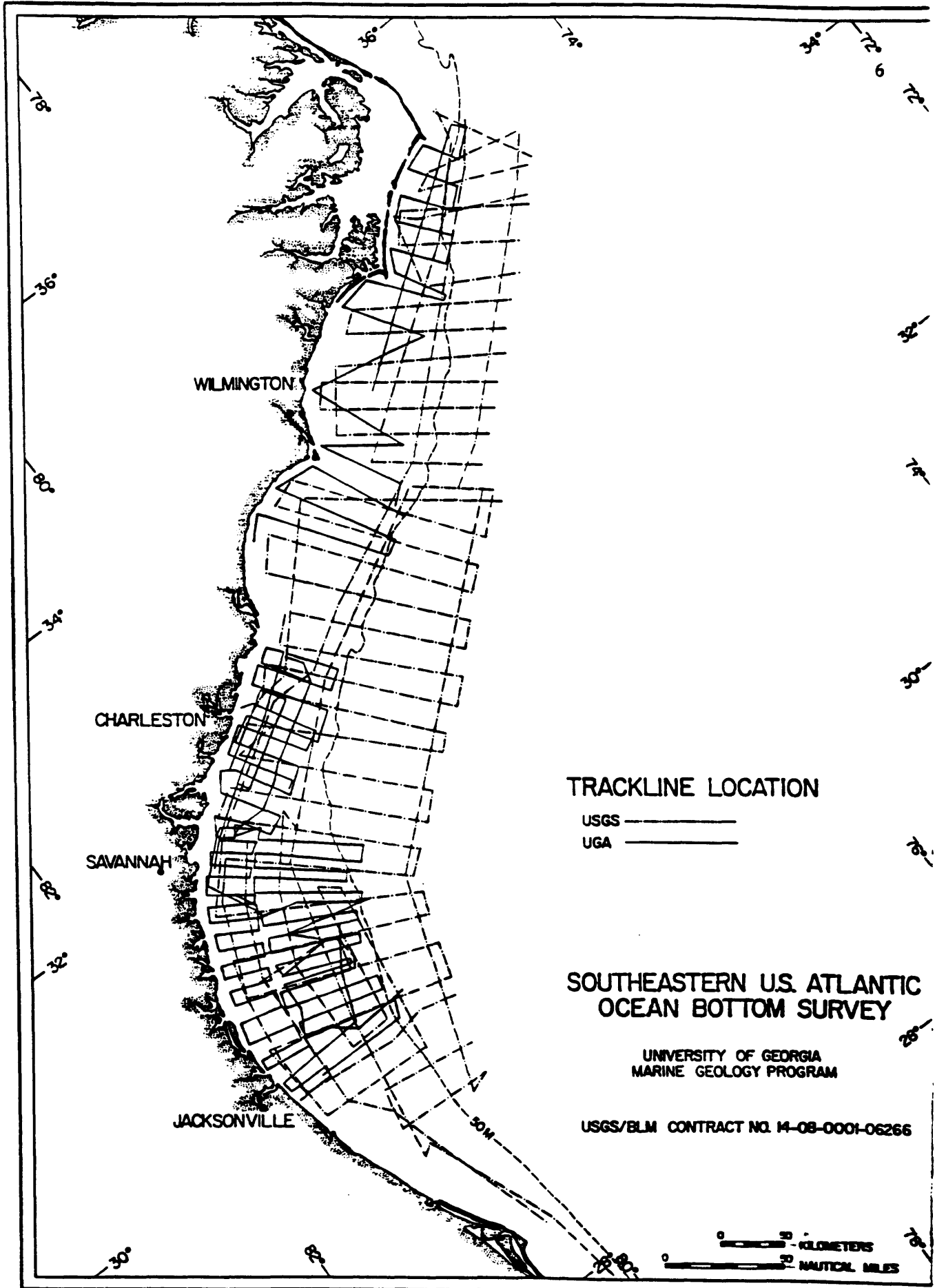


Figure V-2. Tracklines of University of Georgia and USGS seismic-reflection profiles collected under the joint USGS and BLM Environmental Studies program.

81°

80°

7

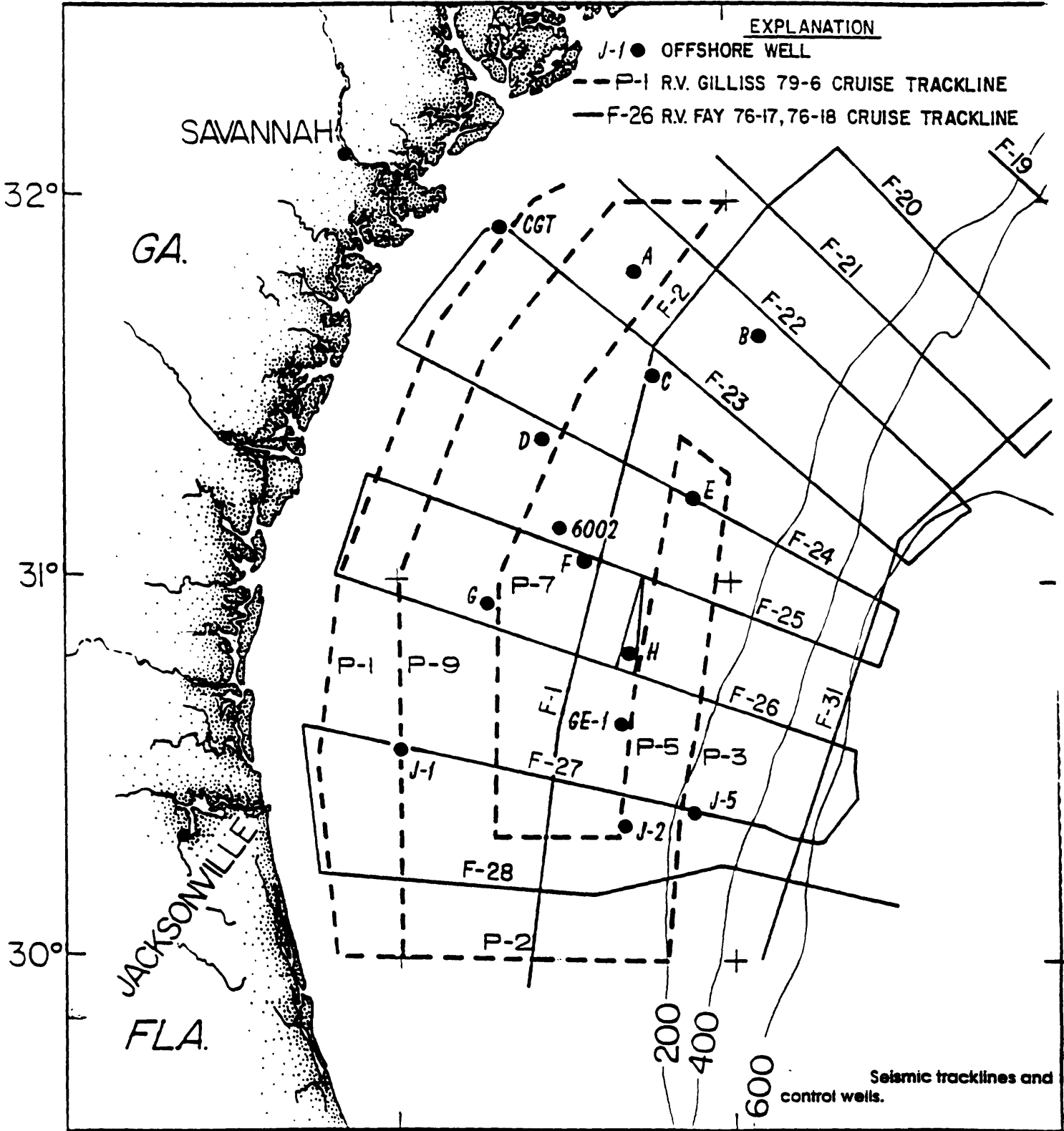


Figure V-3. Cartoon depiction of the paleogeography of the southeastern United States during early Burdigalian deposition.

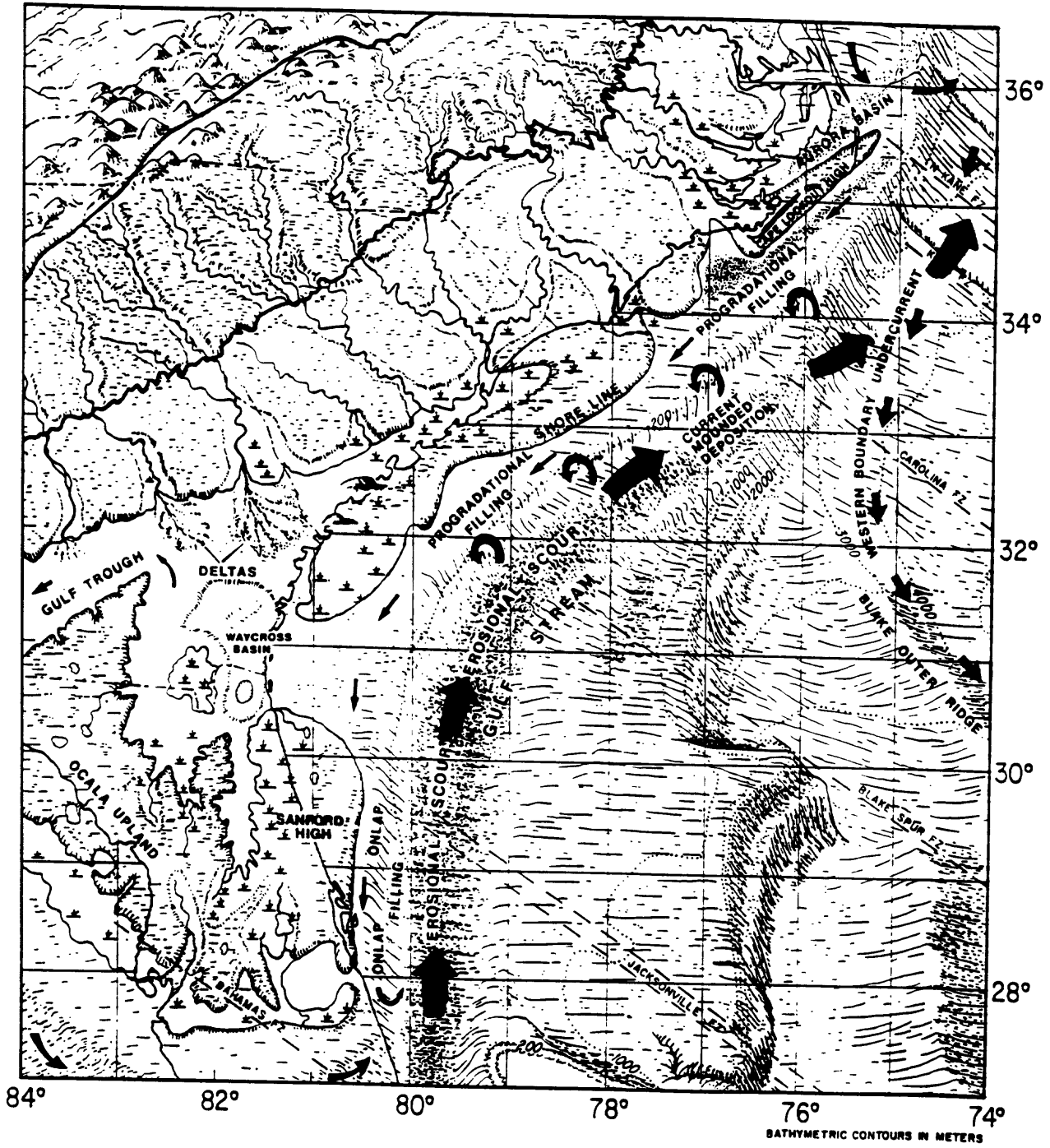
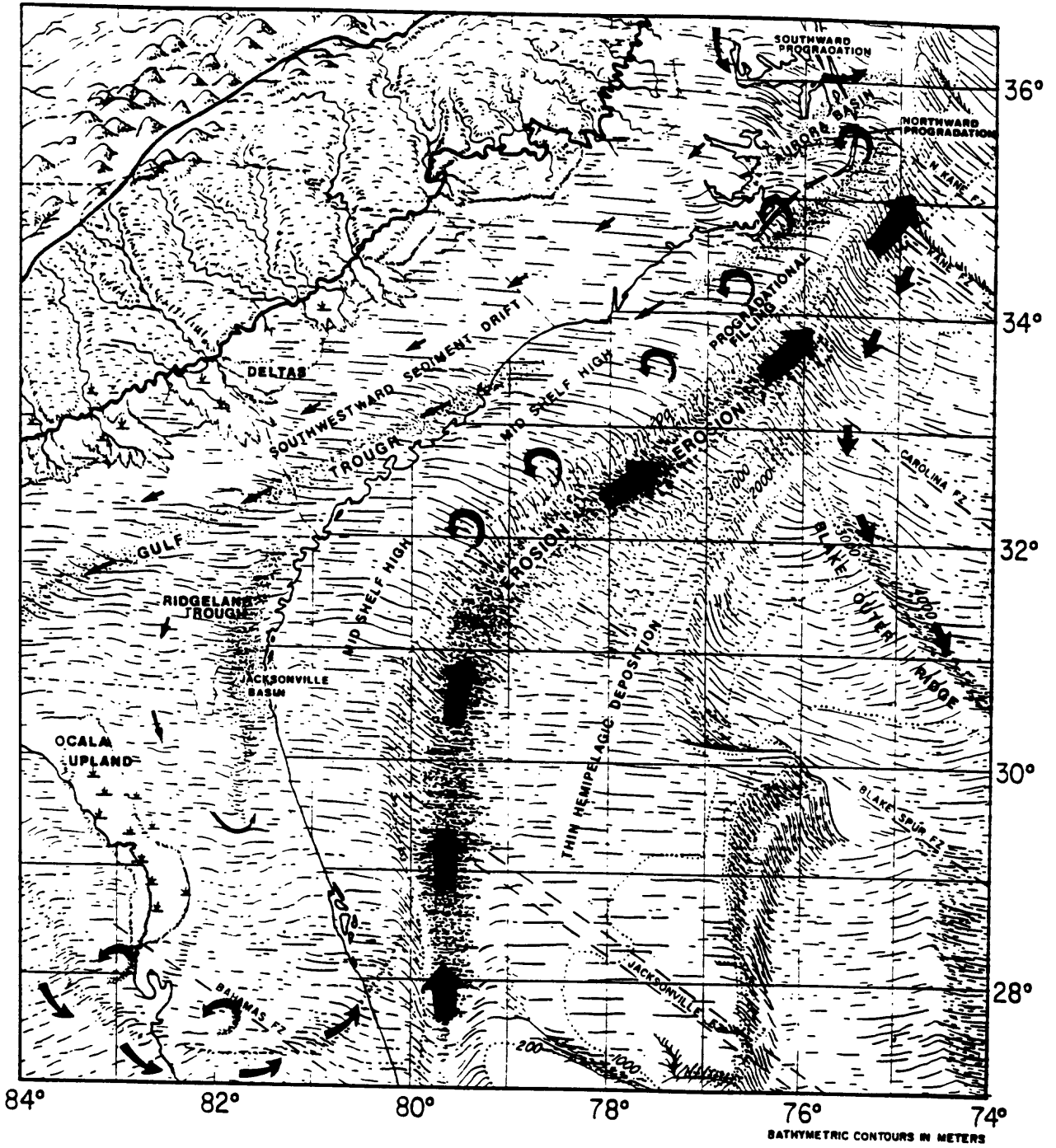


Figure V-4. Cartoon depiction of the Middle Miocene paleogeography of the southeastern United States.



Boreholes B and 6002 penetrated Aquitanian-age sediments equivalent to the lower Parachucla of onshore Georgia (P.F. Huddlestun, unpubl. data, 1988). Under the shelf, these sediments consist of olive silty clay and brownish-olive sandy calcarenite deposited in a shallow marine environment. The unit contains up to 10% phosphorite, with enrichments along the underlying and overlying unconformities.

Sea level fell at the close of the Aquitanian causing a regional unconformity and a change in sedimentation rates and type across much of central Georgia and across the continental shelf. The unconformity under the continental shelf is visible on the seismic-reflection profiles across the Georgia Bight, but is not as pronounced as the late Burdigalian, Langhian, and late Miocene unconformities. Enriched phosphorite zones occur at the unconformity in Borehole D, and the Savannah Light Tower, but the unconformity does not appear to be phosphatic in Borehole B. The lack of a phosphorite zone in Borehole B may be due to a lack of samples at the unconformity.

Burdigalian (middle and upper Early Miocene)

The second major sea-level rise began in the Burdigalian. Central and eastern Georgia during the Burdigalian were still a low area relict from oceanographic events of the Late Cretaceous, Paleocene, and Eocene (the Waycross basin of Popenoe, 1986) and occupied by a seaway that connected the Atlantic with the Gulf of Mexico (Fig. V-3). During the Burdigalian, much of this seaway became filled in central Georgia with poorly sorted sands and silts that represent deltaic deposits (Torreya Formation of Huddlestun, 1982) from the ancestral Ocmulgee, Oconee, and Ogeechee Rivers (Weaver and Beck, 1977). Deltaic deposits grade eastward in Georgia into into fine- to coarse-grained sands with scattered beds of pebbles deposited as shallow-water deltas, and farther east and beneath the continental shelf into phosphatic sands, clays, and interbedded dolomites of estuarine or restricted marine character (equivalent to the Marks Head Formation of Huddlestun, 1982). On the Georgia shelf these Burdigalian age sediments were penetrated in the JOIDES-1, JOIDES- 2, Borehole D, and are probably present but are not recognized at the GE-1 well.

The Burdigalian section drilled in Borehole D and in J-2 has enriched phosphorite zones of about 20% off Georgia. Burdigalian age beds within the Pungo River Formation of North Carolina are mined for phosphorite at the Lee Creek Mine in the Aurora Basin. Riggs and others (1985) show that these same strata off North Carolina in Onslow Bay (FPF-1) contain beds that contain up to 40% phosphorite. In both Borehole D and in the Onslow Bay deposits, the richest Burdigalian phosphorite beds occur just above the unconformity that separates the two major Lower Miocene units, the Aquitanian and Burdigalian, indicating that this enrichment is probably due to reworking at the unconformity. Although the exact location of the Aquitanian-Burdigalian unconformity has not been published for J-2, it probably is at 350 ft where there is a phosphorite enrichment of 30%. A minor sea-level fall at the close of the Burdigalian (Haq and others, 1987) is expressed as an unconformity across much of the continental shelf along which Burdigalian age sediments were removed in 6002, Borehole B, and JOIDES 1.

Langhian (early Middle Miocene)

The Langhian represents the third major sea-level rise of the Miocene, during which seas reached levels of over 150 m above present (Haq and others, 1987). Sediments of Langhian age are poorly preserved in Georgia because of a sea-level fall at the close of the Langhian, during which much of the Langhian sediments

were removed. The Langhian section (lower Middle Miocene) is absent or has not been identified in the TACTS cores, but was identified in JOIDES 1, GE-1, and 6002 off Georgia (Poag and Hall, 1979); a thick section is present in Onslow Bay off North Carolina. Off North Carolina, the Langhian sediments consist of clean quartz sands interbedded with muds deposited in an outer-shelf to upper-slope environment (Katrosch and Snyder, 1982). The sediments are phosphatic but at present have not been identified as mineable resource. In Florida, however, the unit forms the lower part of the Peace River Formation (Scott, 1985), which contains quartz sand beds having greater than 50% phosphorite.

Haq and others (1987) indicate that seas fell at the end of the Langhian to about 50 m above present. This event no doubt created the unconformity along which the Langhian strata were removed at the TACTS core sites and across much of eastern Georgia.

Serravallian (middle Middle Miocene)

Seas again rose in the lower Serravallian to nearly the height of Langhian seas (Haq and others, 1987). A thick and phosphatic lower Serravallian section of carbonate muds, clays, and sands was cored at TACTS boreholes B, D, and H, and at 6002. Serravallian age strata are the most phosphatic unit in offshore Georgia and are equivalent to the onshore phosphatic Berryville Clay Member of the Coosawhatchie Formation. The Berryville Clay member is present near the Coast of Georgia. The unit grades westward into a more clastic and non-phosphatic facies called the Ebenezer Member (Huddlestun, in press). In onshore Georgia, these beds represent deltaic-lacustrine, littoral, and neritic environments (terrigenous to middle shelf marine) (Abbott, 1974). On the continental shelf, in the section drilled by the TACTS cores and at the COST GE-1 well is a deeper water, outer-shelf to upper-slope facies containing mainly planktonic foraminifera (Poag and Hall, 1979, Huddlestun, personal comm, 1988).

The Coosawhatchie Formation of Georgia is equivalent to the upper part of the phosphatic Peace River Formation of Florida and the upper Pungo River Formation of North Carolina. In Onslow Bay, Riggs and others (1985) have shown that this unit probably represents a mineable resource, constituting their BBF-1 to BBF-8 units. BBF-1 lies on the Langhian-Serravallian unconformity and contains phosphorite layers as rich as "75%". The phosphatic layer in Borehole D and 6002, which occurs near the middle of the Serravallian section and contain sand layers with phosphorite over 50%, may be equivalent to Riggs and others (1985) unit BBF-6. Seismic reflection line GYRE 7-P (Fig. V-1) passes near both Borehole D and 6002. Although the lithologies are different in the two wells (sand in Borehole D, and clay in 6002), the phosphatic zone appears to be exactly the same age, occurring along a minor unconformity at both wells. A reflection that probably represents this horizon can be traced between the two wells indicating that we will be able to trace this unit regionally when the remaining TACTS boreholes are logged.

The Upper Miocene unconformity

A pronounced major unconformity representing the upper Middle, and lower Upper Miocene (upper Serravallian and lower Tortonian) truncates and deeply incises the top of the Middle Miocene strata under the shelf and has removed Middle Miocene strata entirely in some areas. As shown in seismic profiles by Kellam and Henry (1986) and unpublished USGS profiles held by Popenoe, this surface represents an extensive subaerial erosion surface. Kellam and Henry (1986) suggest that winnowing and concentration of phosphatic material could have

occurred along this major unconformity, concentrating phosphorite in stream channels and topographic lows. They have also suggested that erosional holes observed in seismic profiles southeast of the Savannah Light Tower at the apex of a regional high on the Miocene top would be primary exploration targets. From all available evidence, the authors of this chapter agrees with that observation.

Evidence for enrichment of phosphorite along the Upper Miocene unconformity is provided by the sand layer with over 70% phosphorite at the Upper Miocene unconformity at Borehole B. Reworked residual phosphorites at the unconformity are probably responsible for the enrichment. Similarly, much of the phosphorite enrichment at the Savannah Light Tower well is probably due to enrichment at the Upper Miocene unconformity.

Southwest of Borehole B, between Borehole B and 6002, there is a regional high (mentioned previously) where the upper Miocene unconformity has stripped away essentially all middle Miocene sediments. This area is highly attractive as an exploration target since the Miocene is shallow, and Miocene sediments have been extensively reworked. We should be able to farther evaluate the potential of this area when Boreholes A and C are logged.

The phosphorite zone penetrated at 6002 is truncated by the Upper Miocene unconformity along seismic line P-7 (Fig. V-1) about 4 miles south of the well. This is another area where the Upper Miocene unconformity could have reworked and possibly enriched the phosphorite zone. Alternatively, the phosphorite may have been completely eroded away along the unconformity. The logging of TACTS Borehole G will help resolve this uncertainty.

The area of Boreholes F, G, and H, is less attractive as an exploration target than to the north, however, because the Miocene sediments are more deeply buried beneath a thick prograding blanket of Pliocene sand and clay. The Miocene strata in this area are, however, reachable by borehole mining techniques.

Tortonian-Messinian (Upper Miocene)

Over most of Georgia the upper Miocene is expressed as an erosional hiatus. Well 6002 off Georgia cored 10 m of olive silty clay topped by dark, grayish-brown phosphatic sand containing late Serravallian and late Miocene diatoms (Abbott, in Hathaway and others, 1979). C.W. Poag (personal comm., 1986) identified N-17 foraminifera (late Tortonian-Messinian) in these same sediments, suggesting that the unit is equivalent in age to part of the phosphatic Peace River and Bone Valley Formations of central Florida. The upper Miocene unit occurs only on the west flank of the midshelf high (Kellam and Henry, 1986, Popenoe, 1986) and is the erosional remnant of a more extensive blanket of late Miocene sediments that once covered most of southern Georgia and Florida before being removed by subaerial erosion in the latest Miocene (Messinian) low sea-level stand. The late Miocene strata under the Georgia shelf do not appear to be notably phosphorite-rich from the available well data.

VI Summary and Conclusions

- 1) Phosphorite is well developed in Neogene (lower to middle Miocene and younger) strata off Georgia, reaching values as high as 21.6% P_2O_5 (47.2 % BPL) in enriched zones. Approximately eighteen separate core samples yielded about 10% volume percent phosphorite pellets or more, even though the sample coverage is estimated to make up only about 8% or less of original penetrated strata.
- 2) All of the high phosphate zones ($\geq 30\%$ pellets) occur at or near major unconformities, presumably due to reworking and winnowing-out of fines and dissolution of carbonates. However, not all unconformities have phosphorite enrichments. The upper middle Miocene (Serravallian to post-Miocene) unconformity is the most extensively developed at the B as well as Savannah Light sites in the northern part of the area, whereas a major unconformity with strong phosphorite enrichment occurs in sites D and AMCOR 6002 in the Serravallian in the central area. This phosphorite zone and its pellet concentrations corresponds well with similar horizons off North Carolina.

The lower Miocene (Aquitanean-Burdigalian) was not penetrated in Borehole H in the central southern part of the region. Phosphorite enrichments are found in these stratigraphic horizons at JOIDES sites J-1 and J-2 in the Florida offshore so should be sought in Georgia as well. The maximum thickness of the zones cannot be established in most cases because of sample sparsity.

- 3) Many of the observed pellets show evidences of primary (in situ) formation, but undeformed pellets along with larger recrystallized phosphorite grains occur in post middle Miocene strata in the upper 15 to 70 m of the holes. We presume that this material is reworked from underlying formations.
- 4) Phosphate-bearing formations correlate well with those in stratigraphic test borings off Florida as well as offshore North Carolina vibracores studied by Riggs and his coworkers (Riggs and others, 1985) indicating that the Georgia offshore deposits are part of a continuous phosphorite depositional environment in the Southeastern United States.
- 5) In the northern area, the uppermost phosphate-enriched zones may be reachable by dredging, utilizing the new Zellars-Williams offshore mining model. However, virtually all the phosphatic Neogene and part of the phosphatic upper Oligocene is probably within borehole mining reach, because of the relatively flat-lying nature of the strata off Georgia. Further evaluations will be required to determine the bearing capacity of strata overlying the phosphate-enriched horizons for borehole mining, as well as the environmental issues associated with mining.
- 6) Many questions remain to be answered. We cannot determine the maximum thickness of phosphorite-enriched layers. More information on the phosphorite concentration and distribution, coupled with the existing seismic data, is needed to place limits on the extent of the phosphorite resources off Georgia, especially in nearer shore areas. Key topics include learning whether residual phosphorite lag deposits remain where seismic data show total absence of phosphatic parent beds determining whether phosphorite enrichment occurs in the lower Miocene.

References Cited

- Abbott, W.H., 1974. Lower Middle Miocene diatom assemblages from the Coosawhatchie Clay Member of the Hawthorne Formation, Jasper County, South Carolina: South Carolina Division of Geology Geologic Notes, v. 18, p. 46-53.
- Charm, W. B., Nesteroff, W. D., and Valides, S., 1969, Detailed stratigraphic description of the JOIDES cores on the continental margin off Florida: U.S. Geological Survey Professional Paper 501-D, p. D1-D13.
- Hathaway, J. C., and others 1979, U.S. Geological Survey core drilling on the Atlantic Shelf: Science v. 206, no. 4418, p. 515-527.
- Haq, B.V., Hardenbol, J., and Vail, P.R., 1987, Chronology of fluctuating sea levels since the Triassic: Science, v. 235, p. 1156-1167.
- Huddlestun, P.F., 1982, The stratigraphic subdivision of the Hawthorne Group of Georgia, in Scott, T.M., and Upchurch, S.B., eds., Miocene of the southeastern United States: Florida Bureau of Geology Special Publication 25, p. 183-184.
- Huddlestun, P.F., 1988, A revision of the lithostratigraphic units of the Coastal Plain of Georgia: Georgia Geologic Survey Bull. 104, 162 p with maps.
- Katrosch, M.R. and Snyder, S.W., 1982, Diagnostic foraminifera and paleoecology of the Pungo River Formation, central Coastal Plain of North Carolina: Southeastern Geology, v. 23, p. 217-232.
- Kellam, J. A., and Henry, V. J., 1986, Interpretation of the seismic stratigraphy of the phosphatic Middle Miocene of the Georgia continental shelf; Georgia Geologic Survey Geologic Atlas 4, 9 plates.
- Marvasti, A., and Riggs, S. R., 1987, Potential for Marine Mining of Phosphate within the U.S. Exclusive Economic Zone (EEZ), Marine Mining, v. 6, p. 291-300.
- McCullum, M. J., and Herrick, S. M., 1964, Offshore extension of the Upper Eocene to Recent stratigraphic sequence in southeastern Georgia; U.S. Geological Survey Professional Paper 501-C, p. C61-C63.
- Pilkey, O. H., and Luternauer, J. L., 1967, A North Carolina shelf phosphate deposit of possible commercial interest; Southeastern Geology, v. 8, p. 33-51.
- Poag, C.W., and Hall, R.E., 1979, Foraminiferal biostratigraphy, paleoecology, and sediment accumulation rates. In Scholle, P.A. ed., Geological Studies of the COST GE-1 Well, United States Outer Continental Shelf Area: U.S. Geological Survey Circular 800, p. 49-63.
- Popenoe, P., 1986, Paleogeography and paleoceanography of the Miocene of the southeastern United States, in Burnett, W. C., and Riggs, S. R., eds. World Phosphate Deposits, v. 3, Neogene Phosphorites of the Southeastern United States: Cambridge University Press, (in press).
- Popenoe, P., and Spalding, J.F., 1988, Isopach and structure maps of the Miocene and Post-Miocene sediments in the Southeast Georgia Embayment, Florida-Hatteras Shelf, offshore Georgia. U.S. Geological Survey Open-File Report 88-397, 12 p.
- Poppe, Lawrence J. (Editor), 1981, Data file Atlantic Margin Coring Project (AMCOR) of the U.S. Geological Survey 1981: U.S. Geological Survey Open-File Report-81-239 96 p.
- Riggs, S.R., 1984, Paleocceanographic model of Neogene phosphorite deposition, U.S. Atlantic Continental Margin. Science, v. 223, p. 123-131.
- Riggs, S.R., and Manheim, F.T., 1987, Mineral resources of the U.S. Atlantic continental margin, in Sheridan, R.E., and Grow, J.A. eds., The Atlantic Continental Margin: U.S.; The Geology of North America v. 1- 2, Geological Society of America, p. 501-520.

- Riggs, S.R., Snyder, S.W.P., Hine, A.C., Snyder, S.W., Ellington, M.D., and Mallette, P.M., 1985, Geologic framework of phosphate resources in Onslow Bay, North Carolina continental shelf: *Economic Geology*, v. 80, p. 716-738.
- Savanick, G.A., 1985, Borehole mining of deep phosphate ore in St. Johns County, Florida: *Mining Engineering*, Feb., p. 144-148.
- Scott, L.E., 1982, Borehole mining of phosphate ores: U.S. Bureau of Mines Open File Report 138-32, 215 p, NTIS PB 82-257411.
- Scott, T.M., 1985, The lithostatigraphy of the Central Florida Phosphate District and its southern extension: in Cathcart, J.B., and Scott, T.M. eds., *Florida Land-Pebble Phosphate District: Guidebook for fieldtrip*, Geological Society of America, Orlando, FL, p. 28-37.
- Van Kauwenbergh, S.J., and McClellan, G.H., 1985, Variations in the mineralogy of the Florida phosphate districts. In Cathcart, J.B., and Scott, T.M. (compilers), *Florida land-pebble phosphate district*, Geological Society of America 1985 Annual Meeting Guidebook, p. 39-67.
- Weaver, C.E., and Beck, K.C., 1977, Miocene of the southeastern United States: a model for chemical sedimentation in a perimarine environment: *Sedimentary Geology*, v. 17, 234 p.
- Zellars-Williams 1979, *Phosphates-offshore Georgia and South Carolina*, contract report for U.S. Geological Survey by Zellars-Williams Inc., 157p.
- Zellars-Williams, 1988, *Draft of Final Report: Resource Assessment Study for Georgia Offshore Minerals (in prep)*.